ESAIM: M2AN 56 (2022) 1911–1938
https://doi.org/10.1051/m2an/2022063

ESAIM: Mathematical Modelling and Numerical Analysis
www.esaim-m2an.org

PENALIZATION METHOD FOR THE NAVIER–STOKES–FOURIER SYSTEM

Danica Basarić[1,*], Eduard Feireisl[1], Mária Lukáčová-Medviďová[2], Hana Mizerová[1,3] and Yuhuan Yuan[2]

Abstract. We apply the method of penalization to the Dirichlet problem for the Navier–Stokes–Fourier system governing the motion of a general viscous compressible fluid confined to a bounded Lipschitz domain. The physical domain is embedded into a large cube on which the periodic boundary conditions are imposed. The original boundary conditions are enforced through a singular friction term in the momentum equation and a heat source/sink term in the internal energy balance. The solutions of the penalized problem are shown to converge to the solution of the limit problem. In particular, we extend the available existence theory to domains with rough (Lipschitz) boundary. Numerical experiments are performed to illustrate the efficiency of the method.

Mathematics Subject Classification. 35A01, 76M12, 76N06.

Received January 7, 2022. Accepted July 18, 2022.

1. Introduction

Let us consider the *Navier–Stokes–Fourier system* in the entropy formulation,

$$\partial_t \varrho + \mathrm{div}_x(\varrho \boldsymbol{u}) = 0, \tag{1.1}$$

$$\partial_t(\varrho \boldsymbol{u}) + \mathrm{div}_x(\varrho \boldsymbol{u} \otimes \boldsymbol{u}) + \nabla_x p = \mathrm{div}_x \mathbb{S}, \tag{1.2}$$

$$\partial_t(\varrho s) + \mathrm{div}_x(\varrho s \boldsymbol{u}) + \mathrm{div}_x\left(\frac{\boldsymbol{q}}{\vartheta}\right) = \frac{1}{\vartheta}\left(\mathbb{S} : \mathbb{D}_x \boldsymbol{u} - \frac{\boldsymbol{q} \cdot \nabla_x \vartheta}{\vartheta}\right). \tag{1.3}$$

The unknowns are the standard variables: the density $\varrho = \varrho(t,x)$, the temperature $\vartheta = \vartheta(t,x)$, and the velocity $\boldsymbol{u} = \boldsymbol{u}(t,x)$, whereas the thermodynamic functions: the pressure $p = p(\varrho, \vartheta)$, the entropy $s = s(\varrho, \vartheta)$ as well as the viscous stress tensor $\mathbb{S} = \mathbb{S}(\vartheta, \mathbb{D}_x \boldsymbol{u})$, and the heat flux $\boldsymbol{q} = \boldsymbol{q}(\vartheta, \nabla_x \vartheta)$ are determined through suitable constitutive relations.

The fluid is confined to a bounded domain $\Omega \subset R^d$, $d = 2, 3$, on the boundary of which the Dirichlet boundary conditions

$$\boldsymbol{u}|_{\partial\Omega} = 0, \ \vartheta|_{\partial\Omega} = \vartheta_B, \ \vartheta_B = \vartheta_B(t,x) \tag{1.4}$$

Keywords and phrases. Navier–Stokes–Fourier system, penalization method, Dirichlet problem, finite volume method.

[1] Institute of Mathematics of the Academy of Sciences of the Czech Republic, Žitná 25, CZ-11567 Praha 1, Czech Republic.

[2] Institute of Mathematics, Johannes Gutenberg-University Mainz, Staudingerweg 9, 55128 Mainz, Germany.

[3] Department of Mathematical Analysis and Numerical Mathematics, Faculty of Mathematics, Physics and Informatics of the Comenius University, Mlynská dolina, 84248 Bratislava, Slovakia.

*Corresponding author: basaric@math.cas.cz

are imposed. Our goal is to approximate solutions of problem (1.1)–(1.4) *via* penalization of the spatial domain. Specifically, we suppose

$$\Omega \subset \mathbb{T}^d,$$

where $\mathbb{T}^d$ is sufficiently large "flat" torus, and replace the field equations (1.1)–(1.3) by the penalized system

$$\partial_t \varrho + \mathrm{div}_x(\varrho \boldsymbol{u}) = 0, \tag{1.5}$$

$$\partial_t(\varrho \boldsymbol{u}) + \mathrm{div}_x(\varrho \boldsymbol{u} \otimes \boldsymbol{u}) + \nabla_x p = \mathrm{div}_x \mathbb{S} - \frac{1}{\varepsilon} \mathbb{1}_{\mathbb{T}^d \setminus \Omega} \boldsymbol{u}, \tag{1.6}$$

$$\partial_t(\varrho s) + \mathrm{div}_x(\varrho s \boldsymbol{u}) + \mathrm{div}_x\left(\frac{\boldsymbol{q}}{\vartheta}\right) = \frac{1}{\vartheta}\left(\mathbb{S} : \mathbb{D}_x \boldsymbol{u} - \frac{\boldsymbol{q} \cdot \nabla_x \vartheta}{\vartheta} - \frac{1}{\varepsilon} \mathbb{1}_{\mathbb{T}^d \setminus \Omega} |\vartheta - \vartheta_B|^k (\vartheta - \vartheta_B)\right) \tag{1.7}$$

on the set $(0,T) \times \mathbb{T}^d$, where ϑ_B is a smooth extension of the boundary temperature on $\mathbb{T}^d \setminus \overline{\Omega}$. Obviously, solving the problem on the flat torus $\mathbb{T}^d$ is equivalent to imposing the space periodic boundary conditions. The solution of the original problem is then recovered by letting $\varepsilon \to 0$ in (1.6), (1.7).

The penalization method is a popular simulation tool when the boundary of Ω has a complicated structure and its approximation by polygons may be problematic. The difficulty with domain approximation and construction of a suitable mesh is transformed to the forcing terms that are much easier to handle. This idea has been used quite often in the literature. Domain penalization is realized in the immersed boundary method [17, 18] and the (Lagrange-multiplier based) fictitious domain method [8, 9, 12]. Both approaches have been originally developed in the context of incompressible Navier–Stokes equations. In the context of fluid-structure interaction problem a penalization method is applied on a moving domain in [2]. Penalization of boundary conditions in a spectral method approximating one- and multidimensional compressible Navier–Stokes–Fourier equations was discussed in [10, 11]. Related numerical analysis for one-dimensional heat equation with a singular forcing term was presented in [1]. For elliptic boundary problems the error estimates between the exact solution and (numerical) solutions of L^2- or H^1 penalization problems were presented in [15, 19–21].

Even at the purely theoretical level, penalization can be useful for problems with low regularity (Lipschitz) of the boundary, where suitable approximation by regularization is hampered by the absence of smooth approximate solutions. Our goal in this paper is twofold:

- Using the framework of *weak solutions*, developed in [6] for the penalized problem and, more recently, in [3] for the original Dirichlet problem, we show that weak solutions of (1.5)–(1.7) converge to a weak solution of (1.1)–(1.4) as $\varepsilon \to 0$. In particular, the hypotheses concerning regularity of the spatial domain indispensable in [3] are relaxed.
- We perform numerical experiments illustrating the abstract results.

As far as we are aware, our paper is the first one to provide analytical results as well as finite volume simulations on complex domains for the penalization method applied to the multidimensional Navier–Stokes–Fourier system with inhomogeneous Dirichlet boundary conditions for the temperature. Possible applications include the celebrated and amply studied Rayleigh–Bénard problem in its original compressible setting, *cf. e.g.* Davidson [4]. The penalization method can efficiently handle domains with rough (Lipschitz) boundaries extending the current theory presented in [3] restricted to smooth domains.

The rest of the paper is organized in the following way: In Section 2 we define the concept of weak solution to the Dirichlet problem for the Navier–Stokes–Fourier system and formulate the main theoretical result on the strong convergence of the penalized solutions. Sections 3 and 4 are devoted to the derivation of the uniform bounds using the ballistic energy inequality and to the convergence analysis of the penalized solutions, respectively. Section 5 presents a series of numerical simulations illustrating robustness and efficiency of the proposed penalization strategy when solving the Dirichlet problem for the Navier–Stokes–Fourier system in complex domains.

2. Constitutive equations, weak solutions, main theoretical result

Before stating our main analytical result, let us introduce the basic hypotheses imposed on the physical domain and constitutive equations.

2.1. Physical domain

We suppose that $\Omega \subset R^d$, $d = 2, 3$ is a bounded domain with Lipschitz boundary. In addition, we suppose that the boundary datum ϑ_B can be extended on $[0,T] \times \mathbb{T}^d$ in the following way:

$$\begin{aligned} &\vartheta_B \in W^{1,\infty}\big([0,T] \times \mathbb{T}^d\big),\ \vartheta_B \in W^{2,\infty}([0,T] \times \Omega) \cap W^{2,\infty}\big([0,T] \times \big(\mathbb{T}^d \setminus \Omega\big)\big), \\ &\inf \vartheta_B > 0,\ \Delta_x \vartheta_B(t,\cdot) = 0 \quad a.a.\ \text{in } [0,T] \times \Omega. \end{aligned} \tag{2.1}$$

Note that such an extension *always* exists as long as Ω as well as the boundary datum are smooth of class at least $C^{2+\nu}$. Optimal results concerning regularity of Ω can be found in the monograph by Medková [16]. For less regular (Lipschitz) domains, condition (2.1) must be imposed as a hypothesis.

2.2. Constitutive equations

The equations of state interrelating the thermodynamic functions p, s, to the internal energy e are motivated by the existence theory developed in [3]. Specifically, we suppose:

$$p(\varrho,\vartheta) = p_{\rm m}(\varrho,\vartheta) + p_{\rm rad}(\vartheta), \qquad \text{with} \quad p_{\rm m}(\varrho,\vartheta) = \vartheta^{\frac{5}{2}} P\left(\frac{\varrho}{\vartheta^{\frac{3}{2}}}\right), \quad p_{\rm rad}(\vartheta) = \frac{a}{3}\vartheta^4, \tag{2.2}$$

$$e(\varrho,\vartheta) = e_{\rm m}(\varrho,\vartheta) + e_{\rm rad}(\varrho,\vartheta), \quad \text{with} \quad e_{\rm m}(\varrho,\vartheta) = \frac{3}{2}\frac{\vartheta^{\frac{5}{2}}}{\varrho} P\left(\frac{\varrho}{\vartheta^{\frac{3}{2}}}\right), \quad e_{\rm rad}(\varrho,\vartheta) = \frac{a}{\varrho}\vartheta^4, \tag{2.3}$$

$$s(\varrho,\vartheta) = s_{\rm m}(\varrho,\vartheta) + s_{\rm rad}(\varrho,\vartheta), \quad \text{with} \quad s_{\rm m}(\varrho,\vartheta) = \mathcal{S}\left(\frac{\varrho}{\vartheta^{\frac{3}{2}}}\right), \qquad s_{\rm rad}(\varrho,\vartheta) = \frac{4a}{3}\frac{\vartheta^3}{\varrho}, \tag{2.4}$$

where $a > 0$, $P \in C^1[0,\infty)$ satisfies

$$P(0) = 0, \quad P'(Z) > 0 \text{ for } Z \geq 0, \quad 0 < \frac{\frac{5}{3}P(Z) - P'(Z)Z}{Z} \leq c \text{ for } Z \geq 0 \tag{2.5}$$

and

$$\mathcal{S}'(Z) = -\frac{3}{2}\frac{\frac{5}{3}P(Z) - P'(Z)Z}{Z^2}. \tag{2.6}$$

It follows from (2.5) and (2.6) that the functions

$$Z \mapsto \frac{P(Z)}{Z^{\frac{5}{3}}} \text{ and } Z \mapsto \mathcal{S}(Z)$$

are decreasing, and we assume

$$\lim_{Z\to\infty} \frac{P(Z)}{Z^{\frac{5}{3}}} = p_\infty > 0, \tag{2.7}$$

$$\lim_{Z\to\infty} \mathcal{S}(Z) = 0. \tag{2.8}$$

We refer to Chapter 2 of [6] for the physical background of the hypotheses (2.2)–(2.8). In particular, equations (2.7) and (2.8) describe the behaviour of the fluid in the degenerate area, where (2.8) is in agreement with the Third law of thermodynamics.

2.3. Transport terms

We suppose the fluid is Newtonian (linearly viscous), with the viscous stress

$$\mathbb{S}(\vartheta, \mathbb{D}_x \boldsymbol{u}) = \mu(\vartheta)\left(\nabla_x \boldsymbol{u} + \nabla_x^t \boldsymbol{u} - \frac{2}{d}\mathrm{div}_x \boldsymbol{u}\,\mathbb{I}\right) + \eta(\vartheta)\,\mathrm{div}_x \boldsymbol{u}\,\mathbb{I}.$$

Here $\mathbb{D}_x \boldsymbol{u} = (\nabla_x \boldsymbol{u} + \nabla_x^t \boldsymbol{u})/2$ stands for the symmetric velocity gradient.

Similarly, the heat flux is given by Fourier's law

$$\boldsymbol{q}(\vartheta, \nabla_x \vartheta) = -\kappa(\vartheta)\nabla_x \vartheta.$$

As for the transport coefficients μ, η and κ, we suppose they are continuously differentiable functions of temperature ϑ satisfying

$$0 < \underline{\mu}(1+\vartheta) \leq \mu(\vartheta) \leq \overline{\mu}(1+\vartheta), \quad |\mu'(\vartheta)| \leq c \text{ for all } \vartheta \geq 0, \tag{2.9}$$

$$0 \leq \eta(\vartheta) \leq \overline{\eta}(1+\vartheta), \tag{2.10}$$

$$0 < \underline{\kappa}(1+\vartheta^\beta) \leq \kappa(\vartheta) \leq \overline{\kappa}(1+\vartheta^\beta), \quad \beta > 6. \tag{2.11}$$

2.4. Weak solutions

The concept of *weak solution* of the penalized system (1.5)–(1.7) was introduced in [6].

Definition 2.1 (Weak solution of the penalized problem)**.** We say that the trio of functions $[\varrho, \vartheta, \boldsymbol{u}]$ is a *weak solution* of the penalized Navier–Stokes–Fourier system (1.5)–(1.7) with the initial data

$$\varrho(0,\cdot) = \varrho_0,\ (\varrho \boldsymbol{u})(0,\cdot) = \boldsymbol{m}_0,\ \varrho s(\varrho,\vartheta)(0,\cdot) = S_0$$

if the following holds.

(i) *Weak formulation of the continuity equation*: the integral identity

$$-\int_{\mathbb{T}^d} \varrho_0 \varphi(0,\cdot)\,\mathrm{d}x = \int_0^T \int_{\mathbb{T}^d} [\varrho \partial_t \varphi + \varrho \boldsymbol{u} \cdot \nabla_x \varphi]\,\mathrm{d}x\,\mathrm{d}t, \tag{2.12}$$

holds for any $\varphi \in C_c^1([0,T) \times \mathbb{T}^d)$.

(ii) *Weak formulation of the renormalized continuity equation*: for any function

$$b \in C^1[0,\infty),\ b' \in C_c[0,\infty)$$

the integral identity

$$-\int_{\mathbb{T}^d} b(\varrho_0)\varphi(0,\cdot)\,\mathrm{d}x = \int_0^T \int_{\mathbb{T}^d} [b(\varrho)\partial_t \varphi + b(\varrho)\boldsymbol{u} \cdot \nabla_x \varphi + \varphi\ (b(\varrho) - b'(\varrho)\varrho)\mathrm{div}_x \boldsymbol{u}]\,\mathrm{d}x\,\mathrm{d}t \tag{2.13}$$

holds for any $\varphi \in C_c^1([0,T) \times \mathbb{T}^d)$.

(iii) *Weak formulation of the momentum equation*: the integral identity

$$\begin{aligned} -\int_{\mathbb{T}^d} \boldsymbol{m}_0 \cdot \boldsymbol{\varphi}(0,\cdot)\,\mathrm{d}x = &\int_0^T \int_{\mathbb{T}^d} [\varrho \boldsymbol{u} \cdot \partial_t \boldsymbol{\varphi} + (\varrho \boldsymbol{u} \otimes \boldsymbol{u}) : \nabla_x \boldsymbol{\varphi} + p(\varrho,\vartheta)\mathrm{div}_x \boldsymbol{\varphi}]\,\mathrm{d}x\,\mathrm{d}t \\ &- \int_0^T \int_{\mathbb{T}^d} \mathbb{S}(\vartheta, \mathbb{D}_x \boldsymbol{u}) : \mathbb{D}_x \boldsymbol{\varphi}\,\mathrm{d}x\,\mathrm{d}t - \frac{1}{\varepsilon}\int_0^T \int_{\mathbb{T}^d \setminus \Omega} \boldsymbol{u} \cdot \boldsymbol{\varphi}\,\mathrm{d}x\,\mathrm{d}t \end{aligned} \tag{2.14}$$

holds for any $\boldsymbol{\varphi} \in C_c^1([0,T) \times \mathbb{T}^d; R^d)$.

(iv) *Weak formulation of the entropy inequality*: the integral inequality

$$
\begin{aligned}
-\int_{\mathbb{T}^d} S_0\ \varphi(0,\cdot)\,\mathrm{d}x \geq \int_0^T \int_{\mathbb{T}^d} \left[\varrho s(\varrho,\vartheta)\big(\partial_t \varphi + \boldsymbol{u}\cdot\nabla_x\varphi\big) + \frac{\boldsymbol{q}(\vartheta,\nabla_x\vartheta)}{\vartheta}\cdot\nabla_x\varphi \right] \mathrm{d}x\,\mathrm{d}t \\
+ \int_0^T \int_{\mathbb{T}^d} \frac{\varphi}{\vartheta}\left(\mathbb{S}(\vartheta,\mathbb{D}_x\boldsymbol{u}) : \mathbb{D}_x\boldsymbol{u} - \frac{\boldsymbol{q}(\vartheta,\nabla_x\vartheta)\cdot\nabla_x\vartheta}{\vartheta} \right) \mathrm{d}x\,\mathrm{d}t \\
- \frac{1}{\varepsilon}\int_0^T \int_{\mathbb{T}^d\setminus\Omega} \frac{\varphi}{\vartheta}\ |\vartheta-\vartheta_B|^k(\vartheta-\vartheta_B)\,\mathrm{d}x\,\mathrm{d}t
\end{aligned}
\tag{2.15}
$$

holds for any $\varphi \in C_c^1([0,T)\times\mathbb{T}^d)$, $\varphi \geq 0$.

(v) *Total energy balance*: the integral inequality

$$
\begin{aligned}
\psi(\tau)\int_{\mathbb{T}^d}\left(\frac{1}{2}\varrho|\boldsymbol{u}|^2 + \varrho e(\varrho,\vartheta)\right)(\tau,\cdot)\,\mathrm{d}x - \int_0^\tau \partial_t\psi \int_{\mathbb{T}^d}\left[\frac{1}{2}\varrho|\boldsymbol{u}|^2 + \varrho e(\varrho,\vartheta)\right]\mathrm{d}x\mathrm{d}t \\
+ \frac{1}{\varepsilon}\int_0^\tau \psi\int_{\mathbb{T}^d\setminus\Omega}|\boldsymbol{u}|^2\,\mathrm{d}x\,\mathrm{d}t + \frac{1}{\varepsilon}\int_0^\tau \psi\int_{\mathbb{T}^d\setminus\Omega}|\vartheta-\vartheta_B|^k(\vartheta-\vartheta_B)\,\mathrm{d}x\,\mathrm{d}t \\
\leq \psi(0)\int_{\mathbb{T}^d}\left(\frac{1}{2}\frac{|\boldsymbol{m}_0|^2}{\varrho_0} + \varrho_0 e(\varrho_0,S_0)\right)\mathrm{d}x
\end{aligned}
\tag{2.16}
$$

holds for *a.e.* $\tau\in(0,T)$ and any $\psi\in C^1[0,T]$, $\psi\geq 0$.

A suitable concept of a weak solution for the system (1.1)–(1.3) endowed with the Dirichlet boundary conditions (1.4) has been developed only recently in [3].

Definition 2.2 (Weak solution of the Dirichlet problem)**.** We say that the trio of functions $[\varrho,\vartheta,\boldsymbol{u}]$ is a *weak solution* of the Navier–Stokes–Fourier system (1.1)–(1.3), with the Dirichlet boundary conditions (1.4) and the initial data

$$
\varrho(0,\cdot)=\varrho_0,\ \ (\varrho\boldsymbol{u})(0,\cdot)=\boldsymbol{m}_0,\ \ \varrho s(\varrho,\vartheta)(0,\cdot)=S_0
$$

if the following holds.

(i) *Weak formulation of the continuity equation*: the integral identity

$$
-\int_\Omega \varrho_0\varphi(0,\cdot)\,\mathrm{d}x = \int_0^T\int_\Omega [\varrho\partial_t\varphi + \varrho\boldsymbol{u}\cdot\nabla_x\varphi]\,\mathrm{d}x\,\mathrm{d}t,
\tag{2.17}
$$

holds for any $\varphi\in C_c^1\big([0,T)\times\overline{\Omega}\big)$.

(ii) *Weak formulation of the renormalized continuity equation*: for any function

$$
b\in C^1[0,\infty),\ b'\in C_c[0,\infty),
$$

the integral identity

$$
-\int_\Omega b(\varrho_0)\varphi(0,\cdot)\,\mathrm{d}x = \int_0^T\int_\Omega [b(\varrho)\partial_t\varphi + b(\varrho)\boldsymbol{u}\cdot\nabla_x\varphi + \varphi\ (b(\varrho)-b'(\varrho)\varrho)\mathrm{div}_x\boldsymbol{u}]\,\mathrm{d}x\,\mathrm{d}t
\tag{2.18}
$$

holds for any $\varphi\in C_c^1\big([0,T)\times\overline{\Omega}\big)$.

(iii) *Weak formulation of the momentum equation*: the integral identity

$$
\begin{aligned}
-\int_\Omega \boldsymbol{m}_0\cdot\boldsymbol{\varphi}(0,\cdot)\,\mathrm{d}x = \int_0^T\int_\Omega [\varrho\boldsymbol{u}\cdot\partial_t\boldsymbol{\varphi} + (\varrho\boldsymbol{u}\otimes\boldsymbol{u}) : \nabla_x\boldsymbol{\varphi} + p(\varrho,\vartheta)\mathrm{div}_x\boldsymbol{\varphi}]\,\mathrm{d}x\,\mathrm{d}t \\
- \int_0^T\int_\Omega \mathbb{S}(\vartheta,\mathbb{D}_x\boldsymbol{u}) : \mathbb{D}_x\boldsymbol{\varphi}\,\mathrm{d}x\,\mathrm{d}t
\end{aligned}
\tag{2.19}
$$

holds for any $\boldsymbol{\varphi}\in C_c^1\big([0,T)\times\Omega;R^d\big)$.

(iv) *Weak formulation of the entropy inequality*: the integral inequality

$$
\begin{aligned}
-\int_\Omega S_0\ \varphi(0,\cdot)\,\mathrm{d}x \geq \int_0^T \int_\Omega \left[\varrho s(\varrho,\vartheta)\big(\partial_t\varphi + \boldsymbol{u}\cdot\nabla_x\varphi\big) + \frac{\boldsymbol{q}(\vartheta,\nabla_x\vartheta)}{\vartheta}\cdot\nabla_x\varphi\right]\mathrm{d}x\,\mathrm{d}t \\
+\int_0^T\int_\Omega \frac{\varphi}{\vartheta}\left(\mathbb{S}(\vartheta,\mathbb{D}_x\boldsymbol{u}):\mathbb{D}_x\boldsymbol{u} - \frac{\boldsymbol{q}(\vartheta,\nabla_x\vartheta)\cdot\nabla_x\vartheta}{\vartheta}\right)\mathrm{d}x\,\mathrm{d}t
\end{aligned}
\tag{2.20}
$$

holds for any $\varphi \in C_c^1([0,T)\times\Omega)$, $\varphi \geq 0$.

(v) *Ballistic energy balance*: for any

$$
\tilde\vartheta \in C^1\big([0,T]\times\overline{\Omega}\big),\ \inf\tilde\vartheta > 0,\ \tilde\vartheta|_{\partial\Omega} = \vartheta_B \tag{2.21}
$$

the integral inequality

$$
\begin{aligned}
\int_\Omega\left(\frac{1}{2}\varrho|\boldsymbol{u}|^2 + \varrho e(\varrho,\vartheta) - \tilde\vartheta\varrho s(\varrho,\vartheta)\right)(\tau,\cdot)\,\mathrm{d}x + \int_0^\tau\int_\Omega \frac{\tilde\vartheta}{\vartheta}\left(\mathbb{S}(\vartheta,\mathbb{D}_x\boldsymbol{u}):\mathbb{D}_x\boldsymbol{u} - \frac{\boldsymbol{q}(\vartheta,\nabla_x\vartheta)\cdot\nabla_x\vartheta}{\vartheta}\right)\mathrm{d}x\,\mathrm{d}t \\
\leq \int_\Omega\left(\frac{1}{2}\frac{|\boldsymbol{m}_0|^2}{\varrho_0} + \varrho_0 e(\varrho_0,S_0) - \tilde\vartheta(0,\cdot)S_0\right)\mathrm{d}x \\
-\int_0^\tau\int_\Omega\left[\varrho s(\varrho,\vartheta)\Big(\partial_t\tilde\vartheta + \boldsymbol{u}\cdot\nabla_x\tilde\vartheta\Big) + \frac{\boldsymbol{q}(\vartheta,\nabla_x\vartheta)\cdot\nabla_x\tilde\vartheta}{\vartheta}\right]\mathrm{d}x\,\mathrm{d}t
\end{aligned}
\tag{2.22}
$$

holds for *a.e.* $\tau\in(0,T)$.

Apparently, the main difference between the two concepts of weak solutions is the total, ballistic energy balance (2.16), (2.22), respectively. In addition, the pointwise inequality (2.22) is weaker than its counterpart (2.16) stated in the differential form. Still (2.22) is sufficient for showing the weak–strong uniqueness property, see [3].

2.5. Main result

Having collected the necessary material, we are ready to state the main theoretical result of the paper.

Theorem 2.3 (Convergence of the penalization method)**.** *Let $\Omega\subset R^d$, $d=2,3$, be a bounded Lipschitz domain. Suppose that the boundary function ϑ_B admits the extension (2.1). Let the thermodynamic functions p, e, s as well as the transport coefficients μ, η, κ satisfy the hypotheses (2.2)–(2.11). Consider a family of measurable initial data*

$$
\varrho_{0,\varepsilon} > 0,\ \boldsymbol{m}_{0,\varepsilon},\ S_{0,\varepsilon}
$$

defined on $\mathbb{T}^d$ and satisfying

$$
\begin{aligned}
\varrho_{0,\varepsilon} &\to \varrho_0 \text{ in } L^1\big(\mathbb{T}^d\big), \\
\boldsymbol{m}_{0,\varepsilon} &\to \boldsymbol{m}_0 \text{ weakly in } L^q\big(\mathbb{T}^d;R^d\big) \text{ for some } q>1, \\
S_{0,\varepsilon} &\to S_0 \text{ weakly in } L^q\big(\mathbb{T}^d\big) \text{ for some } q>1, \\
\int_{\mathbb{T}^d}\left(\frac{1}{2}\frac{|\boldsymbol{m}_{0,\varepsilon}|^2}{\varrho_{0,\varepsilon}} + \varrho_{0,\varepsilon}e(\varrho_{0,\varepsilon},S_{0,\varepsilon})\right)\mathrm{d}x &\to \int_{\mathbb{T}^d}\left(\frac{1}{2}\frac{|\boldsymbol{m}_0|^2}{\varrho_0} + \varrho_0 e(\varrho_0,S_0)\right)\mathrm{d}x
\end{aligned}
\tag{2.23}
$$

as $\varepsilon\to 0$, where

$$
\varrho_0 \geq 0,\ \boldsymbol{m}_0(x) = 0,\ S_0(x) = \varrho_0(x)s(\varrho_0(x),\vartheta_B(x)) \text{ for any } x\in\mathbb{T}^d\setminus\overline{\Omega} \tag{2.24}
$$

if $\vartheta_B = \vartheta_B(x)$ is independent of t;

$$\varrho_0(x) = 0,\ \boldsymbol{m}_0(x) = 0,\ S_0(x) = \varrho_0(x)s(\varrho_0(x), \vartheta_B(0,x)) = \frac{4a}{3}\vartheta_B^3(0,x) \text{ for any } x \in \mathbb{T}^d \setminus \overline{\Omega} \tag{2.25}$$

if $\vartheta_B = \vartheta_B(t,x)$.

Let $(\varrho_\varepsilon, \vartheta_\varepsilon, \boldsymbol{u}_\varepsilon)_{\varepsilon>0}$ *be the corresponding family of weak solutions to the penalized problem specified in Definition 2.1, with the parameter* $k > \beta - 1$.

Then, up to a suitable subsequence,

$$\begin{aligned}
&\varrho_\varepsilon \to \varrho \text{ in } C_{\rm weak}\Big([0,T]; L^{\frac{5}{3}}(\Omega)\Big) \text{ and (strongly) in } L^1((0,T)\times\Omega),\\
&\boldsymbol{u}_\varepsilon \to \boldsymbol{u} \text{ weakly in } L^2\big(0,T; W^{1,2}\big(\Omega; R^d\big)\big),\\
&\vartheta_\varepsilon \to \vartheta \text{ weakly in } L^2\big(0,T; W^{1,2}(\Omega)\big) \text{ and strongly in } L^2((0,T)\times\Omega),
\end{aligned}$$

where $(\varrho, \vartheta, \boldsymbol{u})$ *is a weak solution of the Navier–Stokes–Fourier system* (1.1)–(1.3)*, with the boundary conditions* (1.4) *and the initial conditions* $(\varrho_0, \boldsymbol{m}_0, S_0)$ *in the sense of Definition 2.2.*

Remark 2.4. The existence theory ([6], Chap. 3) can be adapted in a straightforward manner to provide a family of weak solutions $(\varrho_\varepsilon, \vartheta_\varepsilon, \boldsymbol{u}_\varepsilon)_{\varepsilon>0}$ to the penalized problem *assumed* in the hypotheses of Theorem 2.3. Accordingly, Theorem 2.3 represents an alternative proof of existence of a weak solution for the limit system, *cf.* [3].

Remark 2.5. As shown in Section 3.2, formula (3.39) from [6],

$$0 \leq s_m(\varrho, \vartheta) \lesssim 1 + |\log(\varrho)| + [\log(\vartheta)]^+. \tag{2.26}$$

Consequently, we may set

$$\varrho_0 s(\varrho_0, \vartheta_B(0,\cdot)) = \varrho_0 s_m(\varrho_0, \vartheta_B(0,\cdot)) + \frac{4a}{3}\vartheta_B^3(0,\cdot) = \frac{4a}{3}\vartheta_B^3(0,\cdot) \text{ whenever } \varrho_0 = 0$$

in agreement with (2.25)

Remark 2.6. The hypothesis requiring the limit initial density to be zero outside Ω can be dropped provided ϑ_B is independent of time, see Section 4.3.

The forthcoming two sections are devoted to the proof of Theorem 2.3.

3. Uniform bounds

Our goal is to establish uniform bounds for the sequence of solutions of the penalized problem independent of $\varepsilon \to 0$.

3.1. Ballistic energy inequality

The crucial point is rewriting the ballistic energy inequality in terms of the solutions of the penalized problem. To this end, consider

$$\varphi(t,x) = \psi(t)\tilde{\vartheta}(t,x),\ \psi \in C_c^1[0,T),\ \psi \geq 0,$$

where

$$\tilde{\vartheta} \in C^1\big([0,T]\times\mathbb{T}^d\big),\ \inf \tilde{\vartheta} > 0,\ \tilde{\vartheta}|_{\mathbb{T}^d\setminus\Omega} = \vartheta_B \tag{3.1}$$

as a test function in the penalized entropy inequality (2.15). We get

$$\begin{aligned}
-\psi(0)\int_{\mathbb{T}^d} S_{0,\varepsilon}\ \tilde{\vartheta}(0,\cdot)\,\mathrm{d}x \geq{}& \int_0^T \psi \int_{\mathbb{T}^d} \left[\varrho_\varepsilon s(\varrho_\varepsilon,\vartheta_\varepsilon)\Big(\partial_t\tilde{\vartheta} + \boldsymbol{u}_\varepsilon\cdot\nabla_x\tilde{\vartheta}\Big) + \frac{\boldsymbol{q}(\vartheta_\varepsilon,\nabla_x\vartheta_\varepsilon)}{\vartheta_\varepsilon}\cdot\nabla_x\tilde{\vartheta}\right]\mathrm{d}x\,\mathrm{d}t \\
&+ \int_0^T \psi\int_{\mathbb{T}^d}\frac{\tilde{\vartheta}}{\vartheta_\varepsilon}\left(\mathbb{S}(\vartheta_\varepsilon,\mathbb{D}_x\boldsymbol{u}_\varepsilon):\mathbb{D}_x\boldsymbol{u}_\varepsilon - \frac{\boldsymbol{q}(\vartheta_\varepsilon,\nabla_x\vartheta_\varepsilon)\cdot\nabla_x\vartheta_\varepsilon}{\vartheta_\varepsilon}\right)\mathrm{d}x\,\mathrm{d}t \\
&- \frac{1}{\varepsilon}\int_0^T\psi\int_{\mathbb{T}^d\setminus\Omega}\frac{\vartheta_B}{\vartheta_\varepsilon}\,|\vartheta_\varepsilon-\vartheta_B|^k(\vartheta_\varepsilon-\vartheta_B)\,\mathrm{d}x\,\mathrm{d}t \\
&+ \int_0^T \partial_t\psi\int_{\mathbb{T}^d}\varrho_\varepsilon s(\varrho_\varepsilon,\vartheta_\varepsilon)\tilde{\vartheta}\,\mathrm{d}x\,\mathrm{d}t;
\end{aligned}$$

whence, after a straightforward manipulation,

$$\begin{aligned}
-\int_{\mathbb{T}^d} S_{0,\varepsilon}\ \tilde{\vartheta}(0,\cdot)\,\mathrm{d}x \geq{}& \int_0^\tau \int_{\mathbb{T}^d} \left[\varrho_\varepsilon s(\varrho_\varepsilon,\vartheta_\varepsilon)\Big(\partial_t\tilde{\vartheta} + \boldsymbol{u}_\varepsilon\cdot\nabla_x\tilde{\vartheta}\Big) + \frac{\boldsymbol{q}(\vartheta_\varepsilon,\nabla_x\vartheta_\varepsilon)}{\vartheta_\varepsilon}\cdot\nabla_x\tilde{\vartheta}\right]\mathrm{d}x\,\mathrm{d}t \\
&+ \int_0^\tau \int_{\mathbb{T}^d}\frac{\tilde{\vartheta}}{\vartheta_\varepsilon}\left(\mathbb{S}(\vartheta_\varepsilon,\mathbb{D}_x\boldsymbol{u}_\varepsilon):\mathbb{D}_x\boldsymbol{u}_\varepsilon - \frac{\boldsymbol{q}(\vartheta_\varepsilon,\nabla_x\vartheta_\varepsilon)\cdot\nabla_x\vartheta_\varepsilon}{\vartheta_\varepsilon}\right)\mathrm{d}x\,\mathrm{d}t \\
&- \frac{1}{\varepsilon}\int_0^\tau\int_{\mathbb{T}^d\setminus\Omega}\frac{\vartheta_B}{\vartheta_\varepsilon}\,|\vartheta_\varepsilon-\vartheta_B|^k(\vartheta_\varepsilon-\vartheta_B)\,\mathrm{d}x\,\mathrm{d}t \\
&- \int_{\mathbb{T}^d}\varrho_\varepsilon s(\varrho_\varepsilon,\vartheta_\varepsilon)\tilde{\vartheta}(\tau,\cdot)\,\mathrm{d}x \quad \text{for } a.a.\ \tau\in(0,T).
\end{aligned} \tag{3.2}$$

Finally, we subtract (3.2) from the penalized energy balance (2.16) obtaining

$$\begin{aligned}
&\int_{\mathbb{T}^d}\left(\frac{1}{2}\varrho_\varepsilon|\boldsymbol{u}_\varepsilon|^2 + \varrho_\varepsilon e(\varrho_\varepsilon,\vartheta_\varepsilon) - \tilde{\vartheta}\varrho_\varepsilon s(\varrho_\varepsilon,\vartheta_\varepsilon)\right)(\tau,\cdot)\,\mathrm{d}x \\
&\quad+ \int_0^\tau\int_{\mathbb{T}^d}\frac{\tilde{\vartheta}}{\vartheta_\varepsilon}\left(\mathbb{S}(\vartheta_\varepsilon,\mathbb{D}_x\boldsymbol{u}_\varepsilon):\mathbb{D}_x\boldsymbol{u}_\varepsilon - \frac{\boldsymbol{q}(\vartheta_\varepsilon,\nabla_x\vartheta_\varepsilon)\cdot\nabla_x\vartheta_\varepsilon}{\vartheta_\varepsilon}\right)\mathrm{d}x\,\mathrm{d}t \\
&\quad+ \frac{1}{\varepsilon}\int_0^\tau\int_{\mathbb{T}^d\setminus\Omega}\frac{1}{\vartheta_\varepsilon}\,|\vartheta_\varepsilon-\vartheta_B|^{k+2}\,\mathrm{d}x\,\mathrm{d}t + \frac{1}{\varepsilon}\int_0^\tau\int_{\mathbb{T}^d\setminus\Omega}|\boldsymbol{u}_\varepsilon|^2\,\mathrm{d}x\,\mathrm{d}t \\
&\quad\leq \int_{\mathbb{T}^d}\left(\frac{1}{2}\frac{|\boldsymbol{m}_{0,\varepsilon}|^2}{\varrho_{0,\varepsilon}} + \varrho_{0,\varepsilon}e(\varrho_{0,\varepsilon},S_{0,\varepsilon}) - \tilde{\vartheta}(0,\cdot)S_{0,\varepsilon}\right)\mathrm{d}x \\
&\qquad- \int_0^\tau\int_{\mathbb{T}^d}\left[\varrho_\varepsilon s(\varrho_\varepsilon,\vartheta_\varepsilon)\Big(\partial_t\tilde{\vartheta} + \boldsymbol{u}_\varepsilon\cdot\nabla_x\tilde{\vartheta}\Big) + \frac{\boldsymbol{q}(\vartheta_\varepsilon,\nabla_x\vartheta_\varepsilon)\cdot\nabla_x\tilde{\vartheta}}{\vartheta_\varepsilon}\right]\mathrm{d}x\,\mathrm{d}t
\end{aligned} \tag{3.3}$$

for *a.e.* $\tau\in(0,T)$.

3.2. Mass conservation

It follows from the equation of continuity (2.12) that the total mass of the fluid is a constant of motion. Specifically, in accordance with hypothesis (2.25),

$$M_{0,\varepsilon} = \int_{\mathbb{T}^d}\varrho_\varepsilon(\tau,\cdot)\,\mathrm{d}x = \int_{\mathbb{T}^d}\varrho_{0,\varepsilon}\,\mathrm{d}x \to \int_\Omega \varrho_0\,\mathrm{d}x = M_0 \text{ as } \varepsilon\to 0. \tag{3.4}$$

3.3. Energy estimates

In accordance with hypothesis (2.1), we may consider $\tilde{\vartheta} = \vartheta_B$, where ϑ_B is the extension of the boundary temperature specified in (2.1), as a "test" function in the ballistic energy inequality (3.3).

Strictly speaking, equation (3.3) was originally derived for C^1 functions, however, extension of its validity to Lipschitz test functions is straightforward. We obtain

$$\begin{aligned}
&\int_{\mathbb{T}^d}\left(\frac{1}{2}\varrho_\varepsilon|\boldsymbol{u}_\varepsilon|^2+\varrho_\varepsilon e(\varrho_\varepsilon,\vartheta_\varepsilon)-\vartheta_B\varrho_\varepsilon s(\varrho_\varepsilon,\vartheta_\varepsilon)\right)(\tau,\cdot)\,\mathrm{d}x\\
&\quad+\int_0^\tau\int_{\mathbb{T}^d}\frac{\vartheta_B}{\vartheta_\varepsilon}\left(\mathbb{S}(\vartheta_\varepsilon,\mathbb{D}_x\boldsymbol{u}_\varepsilon):\mathbb{D}_x\boldsymbol{u}_\varepsilon-\frac{\boldsymbol{q}(\vartheta_\varepsilon,\nabla_x\vartheta_\varepsilon)\cdot\nabla_x\vartheta_\varepsilon}{\vartheta_\varepsilon}\right)\mathrm{d}x\,\mathrm{d}t\\
&\quad+\frac{1}{\varepsilon}\int_0^\tau\int_{\mathbb{T}^d\setminus\Omega}\frac{1}{\vartheta_\varepsilon}\ |\vartheta_\varepsilon-\vartheta_B|^{k+2}\,\mathrm{d}x\,\mathrm{d}t+\frac{1}{\varepsilon}\int_0^\tau\int_{\mathbb{T}^d\setminus\Omega}|\boldsymbol{u}_\varepsilon|^2\,\mathrm{d}x\,\mathrm{d}t\\
&\quad\leq\int_{\mathbb{T}^d}\left(\frac{1}{2}\frac{|\boldsymbol{m}_{0,\varepsilon}|^2}{\varrho_{0,\varepsilon}}+\varrho_{0,\varepsilon}e(\varrho_{0,\varepsilon},S_{0,\varepsilon})-\vartheta_B(0,\cdot)S_{0,\varepsilon}\right)\mathrm{d}x\\
&\quad\quad-\int_0^\tau\int_{\mathbb{T}^d}\left[\varrho_\varepsilon s(\varrho_\varepsilon,\vartheta_\varepsilon)\Big(\partial_t\vartheta_B+\boldsymbol{u}_\varepsilon\cdot\nabla_x\vartheta_B\Big)+\frac{\boldsymbol{q}(\vartheta_\varepsilon,\nabla_x\vartheta_\varepsilon)\cdot\nabla_x\vartheta_B}{\vartheta_\varepsilon}\right]\mathrm{d}x\,\mathrm{d}t
\end{aligned}\tag{3.5}$$

for *a.e.* $\tau\in(0,T)$.

It follows from the hypotheses (2.9), (2.10) and the Korn–Poincaré inequality (see *e.g.* [6], Prop. 2.1) that

$$\|\boldsymbol{u}_\varepsilon\|^2_{W^{1,2}(\mathbb{T}^d;R^d)}\stackrel{<}{\sim}\int_{\mathbb{T}^d}\frac{\vartheta_B}{\vartheta_\varepsilon}\mathbb{S}(\vartheta_\varepsilon,\mathbb{D}_x\boldsymbol{u}_\varepsilon):\mathbb{D}_x\boldsymbol{u}_\varepsilon\,\mathrm{d}x+\frac{1}{\varepsilon}\int_{\mathbb{T}^d\setminus\Omega}|\boldsymbol{u}_\varepsilon|^2\,\mathrm{d}x.\tag{3.6}$$

Similarly, in accordance with hypothesis (2.11),

$$\left\|\vartheta_\varepsilon^{\frac{\beta}{2}}\right\|^2_{W^{1,2}(\mathbb{T}^d)}+\|\log(\vartheta_\varepsilon)\|^2_{W^{1,2}(\mathbb{T}^d)}\leq c(\vartheta_B)\left[1-\int_{\mathbb{T}^d}\vartheta_B\frac{\boldsymbol{q}(\vartheta_\varepsilon,\nabla_x\vartheta_\varepsilon)\cdot\nabla_x\vartheta_\varepsilon}{\vartheta_\varepsilon^2}\,\mathrm{d}x+\frac{1}{\varepsilon}\int_{\mathbb{T}^d\setminus\Omega}\frac{1}{\vartheta_\varepsilon}\ |\vartheta_\varepsilon-\vartheta_B|^{k+2}\right].\tag{3.7}$$

In view of hypothesis (2.23), the energy of the initial data is uniformly bounded, and we may use (3.6), (3.7) to reduce the inequality (3.5) to

$$\begin{aligned}
&\int_{\mathbb{T}^d}\left(\frac{1}{2}\varrho_\varepsilon|\boldsymbol{u}_\varepsilon|^2+\varrho_\varepsilon e(\varrho_\varepsilon,\vartheta_\varepsilon)-\vartheta_B\varrho_\varepsilon s(\varrho_\varepsilon,\vartheta_\varepsilon)\right)(\tau,\cdot)\,\mathrm{d}x\\
&\quad+\int_0^\tau\left(\|\boldsymbol{u}_\varepsilon\|^2_{W^{1,2}(\mathbb{T}^d;R^d)}+\|\vartheta_\varepsilon^{\frac{\beta}{2}}\|^2_{W^{1,2}(\mathbb{T}^d)}+\|\log(\vartheta_\varepsilon)\|^2_{W^{1,2}(\mathbb{T}^d)}\right)\mathrm{d}t\\
&\quad+\frac{1}{\varepsilon}\int_0^\tau\int_{\mathbb{T}^d\setminus\Omega}\frac{1}{\vartheta_\varepsilon}\ |\vartheta_\varepsilon-\vartheta_B|^{k+2}\,\mathrm{d}x\,\mathrm{d}t+\frac{1}{\varepsilon}\int_0^\tau\int_{\mathbb{T}^d\setminus\Omega}|\boldsymbol{u}_\varepsilon|^2\,\mathrm{d}x\,\mathrm{d}t\\
&\quad\stackrel{<}{\sim}\left[1+\left|\int_0^\tau\int_{\mathbb{T}^d}\left[\varrho_\varepsilon s(\varrho_\varepsilon,\vartheta_\varepsilon)\Big(\partial_t\vartheta_B+\boldsymbol{u}_\varepsilon\cdot\nabla_x\vartheta_B\Big)+\frac{\boldsymbol{q}(\vartheta_\varepsilon,\nabla_x\vartheta_\varepsilon)\cdot\nabla_x\vartheta_B}{\vartheta_\varepsilon}\right]\mathrm{d}x\,\mathrm{d}t\right|\right]
\end{aligned}\tag{3.8}$$

for *a.e.* $\tau\in(0,T)$.

Next, recalling $\Delta_x\vartheta_B=0$ in Ω we may integrate

$$\begin{aligned}
-\int_{\mathbb{T}^d}\frac{\boldsymbol{q}(\vartheta_\varepsilon,\nabla_x\vartheta_\varepsilon)\cdot\nabla_x\vartheta_B}{\vartheta_\varepsilon}\,\mathrm{d}x&=\int_\Omega\frac{\kappa(\vartheta_\varepsilon)\nabla_x\vartheta_\varepsilon\cdot\nabla_x\vartheta_B}{\vartheta_\varepsilon}\,\mathrm{d}x+\int_{\mathbb{T}^d\setminus\Omega}\frac{\kappa(\vartheta_\varepsilon)\nabla_x\vartheta_\varepsilon\cdot\nabla_x\vartheta_B}{\vartheta_\varepsilon}\,\mathrm{d}x\\
&=\int_{\partial\Omega}K(\vartheta_\varepsilon)[\nabla_x\vartheta_B\cdot\boldsymbol{n}\pm]\,\mathrm{d}\sigma_x-\int_{\mathbb{T}^d\setminus\Omega}K(\vartheta_\varepsilon)\Delta_x\vartheta_B\,\mathrm{d}x,
\end{aligned}$$

where we introduced a function K, $K'(\vartheta)=\frac{\kappa(\vartheta)}{\vartheta}$, and where $[\nabla_x\vartheta_B\cdot\boldsymbol{n}\pm]$ denotes a possible jump of the normal derivative of ϑ_B across $\partial\Omega$. As

$$|K(\vartheta_\varepsilon)|\stackrel{<}{\sim}\left(1+|\log(\vartheta_\varepsilon)|+\vartheta_\varepsilon^\beta\right)$$

the volume integral

$$\int_{\mathbb{T}^d\setminus\Omega} K(\vartheta_\varepsilon)\Delta_x\vartheta_B \,\mathrm{d}x$$

is controlled by the left–hand side of (3.8) as soon as $k > \beta - 1$. To control the surface integral, we need the following standard result.

Lemma 3.1. *Let $Q \subset R^d$ be a bounded Lipschitz domain and $\delta > 0$ arbitrary. Then there exists $c(\delta)$ such that*

$$\|v\|^2_{L^2(\partial Q)} \leq \delta \|\nabla_x v\|^2_{L^2(Q;R^d)} + c(\delta)\|v\|^2_{L^2(Q)}$$

for any $v \in W^{1,2}(Q)$.

Proof. Assuming the contrary, we get $\delta_0 > 0$ and sequences $(v_n)_{n=1}^\infty \subset W^{1,2}(Q)$, $C_n \to \infty$ such that

$$\|v_n\|^2_{L^2(\partial Q)} \geq \delta_0 \|\nabla_x v_n\|^2_{L^2(Q;R^d)} + C_n\|v_n\|^2_{L^2(Q)}.$$

Introducing $w_n = v_n/\|v_n\|_{L^2(\partial Q)}$, we get

$$\delta_0\|\nabla_x w_n\|^2_{L^2(Q;R^d)} + C_n\|w_n\|^2_{L^2(Q)} \leq 1,\ \|w_n\|^2_{L^2(\partial Q)} = 1.$$

Consequently, by compactness of the trace operator,

$$w_n \to 0 \text{ weakly in } W^{1,2}(Q) \text{ and } w_n|_{\partial Q} \to 0 \text{ (strongly) in } L^2(\partial Q),$$

which is a contradiction. □

Thus applying Lemma 3.1 to

$$v = \vartheta_\varepsilon^{\frac{\beta}{2}},\ Q = \mathbb{T}^d \setminus \Omega$$

we may infer that the surface integral

$$\int_{\partial\Omega} K(\vartheta_\varepsilon)[\nabla_x\vartheta_B \cdot \boldsymbol{n}\pm]\,\mathrm{d}\sigma_x$$

is controlled by the left–hand side of (3.8).

We conclude by rewriting (3.8) in the form

$$\begin{aligned}
&\int_{\mathbb{T}^d}\left(\frac{1}{2}\varrho_\varepsilon|\boldsymbol{u}_\varepsilon|^2 + \varrho_\varepsilon e(\varrho_\varepsilon,\vartheta_\varepsilon) - \vartheta_B\varrho_\varepsilon s(\varrho_\varepsilon,\vartheta_\varepsilon)\right)(\tau,\cdot)\,\mathrm{d}x \\
&\quad + \int_0^\tau\left(\|\boldsymbol{u}_\varepsilon\|^2_{W^{1,2}(\mathbb{T}^d;R^d)} + \|\vartheta_\varepsilon^{\frac{\beta}{2}}\|^2_{W^{1,2}(\mathbb{T}^d)} + \|\log(\vartheta_\varepsilon)\|^2_{W^{1,2}(\mathbb{T}^d)}\right)\mathrm{d}t \\
&\quad + \frac{1}{\varepsilon}\int_0^\tau\int_{\mathbb{T}^d\setminus\Omega}\frac{1}{\vartheta_\varepsilon}\,|\vartheta_\varepsilon - \vartheta_B|^{k+2}\,\mathrm{d}x\,\mathrm{d}t + \frac{1}{\varepsilon}\int_0^\tau\int_{\mathbb{T}^d\setminus\Omega}|\boldsymbol{u}_\varepsilon|^2\,\mathrm{d}x\,\mathrm{d}t \\
&\quad \lesssim \left[1 + \int_0^\tau\int_{\mathbb{T}^d}\varrho_\varepsilon s(\varrho_\varepsilon,\vartheta_\varepsilon)\left|\partial_t\vartheta_B + \boldsymbol{u}_\varepsilon\cdot\nabla_x\vartheta_B\right|\mathrm{d}x\,\mathrm{d}t\right]
\end{aligned} \tag{3.9}$$

for *a.e.* $\tau \in (0,T)$.

Finally, in accordance with hypothesis (2.4) and by virtue of (2.26),

$$\varrho_\varepsilon s(\varrho_\varepsilon,\vartheta_\varepsilon)|\boldsymbol{u}_\varepsilon| = \varrho_\varepsilon\mathcal{S}\left(\frac{\varrho_\varepsilon}{\vartheta_\varepsilon^{\frac{3}{2}}}\right)|\boldsymbol{u}_\varepsilon| + \frac{4a}{3}\vartheta_\varepsilon^3|\boldsymbol{u}_\varepsilon| \leq \varrho_\varepsilon\mathcal{S}\left(\frac{\varrho_\varepsilon}{\vartheta_\varepsilon^{\frac{3}{2}}}\right)|\boldsymbol{u}_\varepsilon| + \delta|\boldsymbol{u}_\varepsilon|^2 + c(\delta)\vartheta_\varepsilon^6 \tag{3.10}$$

for any $\delta > 0$. Moreover, in accordance with the hypotheses (2.6), (2.8),

$$0 \leq \varrho_\varepsilon \mathcal{S}\left(\frac{\varrho_\varepsilon}{\vartheta_\varepsilon^{\frac{3}{2}}}\right) \lesssim \left(1 + \vartheta_\varepsilon^{\frac{3}{2}}\left(1 + [\log(\vartheta_\varepsilon)]^+\right)\right) \quad \text{if } \frac{\varrho_\varepsilon}{\vartheta_\varepsilon^{\frac{3}{2}}} \leq 1,$$
$$0 \leq \varrho_\varepsilon \mathcal{S}\left(\frac{\varrho_\varepsilon}{\vartheta_\varepsilon^{\frac{3}{2}}}\right) \lesssim \varrho_\varepsilon \quad \text{if } \frac{\varrho_\varepsilon}{\vartheta_\varepsilon^{\frac{3}{2}}} > 1.$$

Thus, going back to (3.9), we conclude

$$\int_{\mathbb{T}^d} \varrho_\varepsilon s(\varrho_\varepsilon, \vartheta_\varepsilon)|\boldsymbol{u}_\varepsilon| \,\mathrm{d}x \lesssim \delta \|\boldsymbol{u}_\varepsilon\|^2_{L^2(\mathbb{T}^d;R^d)} + c(\delta)\|\vartheta_\varepsilon\|^6_{L^6(\mathbb{T}^d)} + \int_{\mathbb{T}^d} \varrho_\varepsilon |\boldsymbol{u}_\varepsilon|^2 \,\mathrm{d}x + M_{0,\varepsilon} \tag{3.11}$$

for any $\delta > 0$.

The bound (3.11) together with (3.9) yield the desired conclusion

$$\begin{aligned}
&\int_{\mathbb{T}^d} \left(\frac{1}{2}\varrho_\varepsilon |\boldsymbol{u}_\varepsilon|^2 + \varrho_\varepsilon e(\varrho_\varepsilon, \vartheta_\varepsilon) - \vartheta_B \varrho_\varepsilon s(\varrho_\varepsilon, \vartheta_\varepsilon)\right)(\tau, \cdot)\,\mathrm{d}x \\
&\quad + \int_0^\tau \left(\|\boldsymbol{u}_\varepsilon\|^2_{W^{1,2}(\mathbb{T}^d;R^d)} + \|\vartheta_\varepsilon^{\frac{\beta}{2}}\|^2_{W^{1,2}(\mathbb{T}^d)} + \|\log(\vartheta_\varepsilon)\|^2_{W^{1,2}(\mathbb{T}^d)}\right) \mathrm{d}t \\
&\quad + \frac{1}{\varepsilon}\int_0^\tau \int_{\mathbb{T}^d \setminus \Omega} \frac{1}{\vartheta_\varepsilon} |\vartheta_\varepsilon - \vartheta_B|^{k+2} \,\mathrm{d}x\,\mathrm{d}t + \frac{1}{\varepsilon}\int_0^\tau \int_{\mathbb{T}^d \setminus \Omega} |\boldsymbol{u}_\varepsilon|^2 \,\mathrm{d}x\,\mathrm{d}t \\
&\quad \lesssim \left[1 + \int_0^\tau \int_{\mathbb{T}^d} \left(\frac{1}{2}\varrho_\varepsilon |\boldsymbol{u}_\varepsilon|^2 + \varrho_\varepsilon e(\varrho_\varepsilon, \vartheta_\varepsilon)\right) \mathrm{d}x\,\mathrm{d}t\right]
\end{aligned} \tag{3.12}$$

for *a.e.* $\tau \in (0, T)$. As the entropy is dominated by the energy, we may use Gronwall's argument to conclude

$$\begin{aligned}
&\operatorname*{ess\,sup}_{\tau \in (0,T)} \int_{\mathbb{T}^d} \left(\frac{1}{2}\varrho_\varepsilon |\boldsymbol{u}_\varepsilon|^2 + \varrho_\varepsilon e(\varrho_\varepsilon, \vartheta_\varepsilon)\right) \mathrm{d}x \lesssim 1, \\
&\int_0^T \left(\|\boldsymbol{u}_\varepsilon\|^2_{W^{1,2}(\mathbb{T}^d;R^d)} + \|\vartheta_\varepsilon^{\frac{\beta}{2}}\|^2_{W^{1,2}(\mathbb{T}^d)} + \|\log(\vartheta_\varepsilon)\|^2_{W^{1,2}(\mathbb{T}^d)}\right) \mathrm{d}t \lesssim 1, \\
&\int_0^T \int_{\mathbb{T}^d \setminus \Omega} \frac{1}{\vartheta_\varepsilon} |\vartheta_\varepsilon - \vartheta_B|^{k+2} \,\mathrm{d}x\,\mathrm{d}t + \int_0^T \int_{\mathbb{T}^d \setminus \Omega} |\boldsymbol{u}_\varepsilon|^2 \,\mathrm{d}x\,\mathrm{d}t \lesssim \varepsilon
\end{aligned} \tag{3.13}$$

uniformly for $\varepsilon > 0$.

4. Convergence

The ultimate step in the proof of Theorem 2.3 is letting $\varepsilon \to 0$ in the sequence of approximate solutions $(\varrho_\varepsilon, \vartheta_\varepsilon, \boldsymbol{u}_\varepsilon)_{\varepsilon > 0}$. We claim that this reduces essentially to performing the limit in the ballistic energy inequality (3.3). Indeed the weak formulation of the equation of continuity is the same for the penalized and the limit system, while the momentum and the entropy balance (2.19), (2.20) do not see the penalization terms in (2.14), (2.15), respectively, as the relevant test functions are compactly supported. Consequently, the limit in the equation of continuity (2.12), the momentum equation (2.14) as well as the entropy inequality (2.15) can be performed using the known compactness arguments as in Chapter 3 of [6]. Thus our task reduces to:

- verifying the renormalized equation of continuity for the limit $(\varrho, \boldsymbol{u})$;
- performing the limit in the ballistic energy inequality (3.3).

In the following text, we focus on the general case of a time dependent $\vartheta_B = \vartheta_B(t, x)$ as specified in hypothesis (2.24). The necessary modifications to handle hypothesis (2.25) are discussed in Section 4.3.

4.1. Renormalized equation of continuity

Basically each step in the following arguments requires passing to a suitable subsequence in the family of approximate solutions we will not relabel for simplicity. First, as a consequence of the hypotheses (2.3), (2.7), we have

$$\varrho^{\frac{5}{3}} + \vartheta^4 \lesssim \varrho e(\varrho, \vartheta).$$

Consequently, in view of the uniform bounds (3.13)

$$\begin{aligned}
\varrho_\varepsilon &\to \varrho \text{ weakly-(*) in } L^\infty\Big(0,T; L^{\frac{5}{3}}\big(\mathbb{T}^d\big)\Big),\\
\vartheta_\varepsilon &\to \vartheta \text{ weakly-(*) in } L^\infty\big(0,T; L^4\big(\mathbb{T}^d\big)\big),\\
\boldsymbol{u}_\varepsilon &\to \boldsymbol{u} \text{ weakly in } L^2\big(0,T; W^{1,2}\big(\mathbb{T}^d; R^d\big)\big),\\
\varrho_\varepsilon \boldsymbol{u}_\varepsilon &\to \overline{\varrho \boldsymbol{u}} \text{ weakly-(*) in } L^\infty\Big(0,T; L^{\frac{5}{4}}\big(\mathbb{T}^d; R^d\big)\Big).
\end{aligned} \tag{4.1}$$

In addition, as $(\varrho_\varepsilon, \boldsymbol{u}_\varepsilon)$ satisfy the equation of continuity (2.12), we get

$$\begin{aligned}
\varrho_\varepsilon &\to \varrho \text{ in } C_{\rm weak}\Big([0,T]; L^{\frac{5}{3}}\big(\mathbb{T}^d\big)\Big),\\
\overline{\varrho \boldsymbol{u}} &= \varrho \boldsymbol{u}.
\end{aligned} \tag{4.2}$$

In particular, the equation of continuity (2.12) is satisfied in $(0,T)\times\mathbb{T}^d$ by the limit $(\varrho, \boldsymbol{u})$.

Next, using (3.13) again we get

$$\boldsymbol{u}_\varepsilon \to 0 \text{ in } L^2\big((0,T)\times\big(\mathbb{T}^d \setminus \Omega\big); R^d\big) \tag{4.3}$$

yielding

$$\boldsymbol{u} \in L^2\Big(0,T; W_0^{1,2}\big(\Omega; R^d\big)\Big).$$

Moreover, as ϱ satisfies the equation of continuity, we get

$$\partial_t \varrho = 0 \text{ in } \mathcal{D}'\big((0,T)\times\big(\mathbb{T}^d \setminus \Omega\big)\big).$$

By virtue of hypothesis (2.25),

$$\varrho(0,\cdot) = \varrho_0 = 0 \text{ in } \mathbb{T}^d \setminus \Omega,$$

and we may infer that

$$\begin{aligned}
&\varrho = 0 \ \text{ in } (0,T)\times\big(\mathbb{T}^d \setminus \Omega\big),\\
&\varrho_\varepsilon \to 0 \text{ in } L^q\big((0,T)\times\big(\mathbb{T}^d \setminus \Omega\big)\big) \text{ for any } 1 \le q < \frac{5}{3}.
\end{aligned} \tag{4.4}$$

We conclude that $(\varrho, \boldsymbol{u}) = (0,0)$ satisfy the renormalized equation of continuity in $(0,T)\times\big(\mathbb{T}^d \setminus \Omega\big)$, while the known arguments yield the same conclusion in $(0,T)\times\Omega$. By the same token, we may suppose

$$\varrho_\varepsilon \to \varrho \text{ (strongly) in } L^q((0,T)\times\Omega) \text{ for any } 1 \le q < \frac{5}{3}. \tag{4.5}$$

4.2. Ballistic energy

Our ultimate goal in the proof of Theorem 2.3 is to perform the limit $\varepsilon \to 0$ in the ballistic energy inequality (3.3). The first issue to discuss is the strong convergence of the temperature. In view of the uniform bounds (3.13), we may suppose

$$\begin{aligned}
\vartheta_\varepsilon &\to \vartheta \text{ weakly in } L^2\big(0,T; W^{1,2}\big(\mathbb{T}^d\big)\big),\\
\log(\vartheta_\varepsilon) &\to \overline{\log(\vartheta)} \text{ weakly in } L^2\big(0,T; W^{1,2}\big(\mathbb{T}^d\big)\big).
\end{aligned} \tag{4.6}$$

In addition, we have strong (*a.a.* pointwise) convergence in Ω by the compactness arguments of Chapter 3 from [6], say,

$$\vartheta_\varepsilon \to \vartheta \text{ (strongly) in } L^2((0,T)\times\Omega),$$

and, again by (3.13),

$$\vartheta_\varepsilon \to \vartheta_B \text{ in } L^{k+1}\big((0,T)\times(\mathbb{T}^d\setminus\Omega)\big). \tag{4.7}$$

Thus we may infer

$$\vartheta_\varepsilon \to \vartheta \text{ in } L^2\big((0,T)\times\mathbb{T}^d\big),\ (\vartheta-\vartheta_B) \text{ in } L^2(0,T;W_0^{1,2}(\Omega)),\ \overline{\log(\vartheta)} = \log(\vartheta), \tag{4.8}$$

in particular, $\vartheta > 0$ *a.a.* in $(0,T)\times\mathbb{T}^d$.

We are ready to perform the limit in the ballistic energy inequality (3.3). To begin, in view of the hypotheses (2.23), (2.25),

$$\int_{\mathbb{T}^d}\left(\frac{1}{2}\frac{|\boldsymbol{m}_{0,\varepsilon}|^2}{\varrho_{0,\varepsilon}} + \varrho_{0,\varepsilon}e(\varrho_{0,\varepsilon},S_{0,\varepsilon}) - \tilde\vartheta(0,\cdot)S_{0,\varepsilon}\right)\mathrm{d}x \to \int_\Omega\left(\frac{1}{2}\frac{|\boldsymbol{m}_0|^2}{\varrho_0} + \varrho_0 e(\varrho_0,S_0) - \tilde\vartheta(0,\cdot)S_0\right)\mathrm{d}x - \int_{\mathbb{T}^d\setminus\Omega}\frac{a}{3}\vartheta_B^4(0,\cdot)\,\mathrm{d}x. \tag{4.9}$$

Similarly, using the strong convergence of $(\varrho_\varepsilon,\vartheta_\varepsilon)$ established in (4.5), (4.7) we get

$$\liminf_{\varepsilon\to 0}\int_{\tau-\delta}^{\tau+\delta}\int_{\mathbb{T}^d}\left(\frac{1}{2}\varrho_\varepsilon|\boldsymbol{u}_\varepsilon|^2 + \varrho_\varepsilon e(\varrho_\varepsilon,\vartheta_\varepsilon) - \tilde\vartheta\varrho_\varepsilon s(\varrho_\varepsilon,\vartheta_\varepsilon)\right)\mathrm{d}x\,\mathrm{d}t \geq \int_{\tau-\delta}^{\tau+\delta}\int_\Omega\left(\frac{1}{2}\varrho|\boldsymbol{u}|^2 + \varrho e(\varrho,\vartheta) - \tilde\vartheta\varrho s(\varrho,\vartheta)\right)\mathrm{d}x\,\mathrm{d}t - \int_{\tau-\delta}^{\tau+\delta}\int_{\mathbb{T}^d\setminus\Omega}\frac{a}{3}\vartheta_B^4\,\mathrm{d}x\,\mathrm{d}t. \tag{4.10}$$

for any $\delta > 0$.

Next, by the same argument,

$$\begin{aligned}
-\int_0^\tau\int_{\mathbb{T}^d}\varrho_\varepsilon s(\varrho_\varepsilon,\vartheta_\varepsilon)\partial_t\tilde\vartheta\,\mathrm{d}x\,\mathrm{d}t &\to -\int_0^\tau\int_\Omega\varrho s(\varrho,\vartheta)\partial_t\tilde\vartheta\,\mathrm{d}x\,\mathrm{d}t - \int_0^\tau\int_{\mathbb{T}^d\setminus\Omega}\frac{4a}{3}\vartheta_B^3\partial_t\vartheta_B\,\mathrm{d}x\,\mathrm{d}t\\
&= -\int_0^\tau\int_\Omega\varrho s(\varrho,\vartheta)\partial_t\tilde\vartheta\,\mathrm{d}x\,\mathrm{d}t - \int_0^\tau\frac{\mathrm{d}}{\mathrm{d}t}\int_{\mathbb{T}^d\setminus\Omega}\frac{a}{3}\vartheta_B^4\,\mathrm{d}x\,\mathrm{d}t\\
&= -\int_0^\tau\int_\Omega\varrho s(\varrho,\vartheta)\partial_t\tilde\vartheta\,\mathrm{d}x\,\mathrm{d}t - \int_{\mathbb{T}^d\setminus\Omega}\frac{a}{3}\vartheta_B^4(\tau,\cdot)\,\mathrm{d}x + \int_{\mathbb{T}^d\setminus\Omega}\frac{a}{3}\vartheta_B^4(0,\cdot)\,\mathrm{d}x.
\end{aligned} \tag{4.11}$$

In addition, by virtue of (4.3),

$$\int_0^\tau\int_{\mathbb{T}^d}\varrho_\varepsilon s(\varrho_\varepsilon,\vartheta_\varepsilon)\boldsymbol{u}_\varepsilon\cdot\nabla_x\tilde\vartheta\,\mathrm{d}x\,\mathrm{d}t \to \int_0^\tau\int_\Omega\varrho s(\varrho,\vartheta)\boldsymbol{u}\cdot\nabla_x\tilde\vartheta\,\mathrm{d}x\,\mathrm{d}t. \tag{4.12}$$

Summing up (4.9)–(4.12) and plugging the result in the ballistic energy inequality (3.3) we obtain

$$\begin{aligned}
&\int_{\tau-\delta}^{\tau+\delta}\int_\Omega\left(\frac{1}{2}\varrho|\boldsymbol{u}|^2 + \varrho e(\varrho,\vartheta) - \tilde\vartheta\varrho s(\varrho,\vartheta)\right)(s,\cdot)\,\mathrm{d}x\,\mathrm{d}s\\
&\quad + \liminf_{\varepsilon\to 0}\int_{\tau-\delta}^{\tau+\delta}\int_0^s\int_{\mathbb{T}^d}\frac{\tilde\vartheta}{\vartheta_\varepsilon}\left(\mathbb{S}(\vartheta_\varepsilon,\mathbb{D}_x\boldsymbol{u}_\varepsilon):\mathbb{D}_x\boldsymbol{u}_\varepsilon - \frac{\boldsymbol{q}(\vartheta_\varepsilon,\nabla_x\vartheta_\varepsilon)\cdot\nabla_x\vartheta_\varepsilon}{\vartheta_\varepsilon}\right)\mathrm{d}x\,\mathrm{d}t\,\mathrm{d}s\\
&\quad \leq 2\delta\int_\Omega\left(\frac{1}{2}\frac{|\boldsymbol{m}_0|^2}{\varrho_0} + \varrho_0 e(\varrho_0,S_0) - \tilde\vartheta(0,\cdot)S_0\right)\mathrm{d}x
\end{aligned}$$

$$- \int_{\tau-\delta}^{\tau+\delta} \int_0^s \int_\Omega \Big(\varrho s(\varrho, \vartheta) \Big(\partial_t \tilde{\vartheta} + \boldsymbol{u} \cdot \nabla_x \tilde{\vartheta} \Big) \Big) \,\mathrm{d}x \,\mathrm{d}t \,\mathrm{d}s$$
$$- \lim_{\varepsilon \to 0} \int_{\tau-\delta}^{\tau+\delta} \int_0^s \int_{\mathbb{T}^d} \frac{\boldsymbol{q}(\vartheta_\varepsilon, \nabla_x \vartheta_\varepsilon) \cdot \nabla_x \tilde{\vartheta}}{\vartheta_\varepsilon} \,\mathrm{d}x \,\mathrm{d}t \,\mathrm{d}s \tag{4.13}$$

for any $\delta > 0$.

Next,

$$\int_{\mathbb{T}^d} \frac{\tilde{\vartheta}}{\vartheta_\varepsilon} \mathbb{S}(\vartheta_\varepsilon, \mathbb{D}_x \boldsymbol{u}_\varepsilon) : \mathbb{D}_x \boldsymbol{u}_\varepsilon \,\mathrm{d}x = \int_{\mathbb{T}^d} \tilde{\vartheta} \mu(\vartheta_\varepsilon) \frac{1}{2\vartheta_\varepsilon} \left| \nabla_x \boldsymbol{u}_\varepsilon + \nabla_x^t \boldsymbol{u}_\varepsilon - \frac{2}{d} \mathrm{div}_x \boldsymbol{u}_\varepsilon \mathbb{I} \right|^2 \mathrm{d}x + \int_{\mathbb{T}^d} \tilde{\vartheta} \eta(\vartheta_\varepsilon) \frac{1}{\vartheta_\varepsilon} |\mathrm{div}_x \boldsymbol{u}_\varepsilon|^2 \,\mathrm{d}x.$$

Consequently, combining convexity of the function

$$(\vartheta, Z) \mapsto \frac{|Z|^2}{\vartheta}$$

with the strong convergence of the temperature established in (4.8), we may infer that

$$\liminf_{\varepsilon \to 0} \int_{\tau-\delta}^{\tau+\delta} \int_0^s \int_{\mathbb{T}^d} \frac{\tilde{\vartheta}}{\vartheta_\varepsilon} \mathbb{S}(\vartheta_\varepsilon, \mathbb{D}_x \boldsymbol{u}_\varepsilon) : \mathbb{D}_x \boldsymbol{u}_\varepsilon \,\mathrm{d}x \,\mathrm{d}t \,\mathrm{d}s \geq \int_{\tau-\delta}^{\tau+\delta} \int_0^s \int_\Omega \frac{\tilde{\vartheta}}{\vartheta} \mathbb{S}(\vartheta, \mathbb{D}_x \boldsymbol{u}) : \mathbb{D}_x \boldsymbol{u} \,\mathrm{d}x \,\mathrm{d}t \,\mathrm{d}s. \tag{4.14}$$

Similarly, we rewrite

$$- \int_{\mathbb{T}^d} \frac{\tilde{\vartheta}}{\vartheta_\varepsilon^2} \boldsymbol{q}(\vartheta_\varepsilon, \nabla_x \vartheta_\varepsilon) \cdot \nabla_x \vartheta_\varepsilon \,\mathrm{d}x = \int_{\mathbb{T}^d} \tilde{\vartheta} \kappa(\vartheta_\varepsilon) |\nabla_x \log(\vartheta_\varepsilon)|^2 \,\mathrm{d}x.$$

Consequently, using arguments similar to (4.14), we get

$$- \liminf_{\varepsilon \to 0} \int_{\tau-\delta}^{\tau+\delta} \int_0^s \int_{\mathbb{T}^d} \frac{\tilde{\vartheta}}{\vartheta_\varepsilon} \frac{\boldsymbol{q}(\vartheta_\varepsilon, \nabla_x \vartheta_\varepsilon) \cdot \nabla_x \vartheta_\varepsilon}{\vartheta_\varepsilon} \,\mathrm{d}x \,\mathrm{d}t \,\mathrm{d}s \geq - \int_{\tau-\delta}^{\tau+\delta} \int_0^s \int_\Omega \frac{\tilde{\vartheta}}{\vartheta} \frac{\boldsymbol{q}(\vartheta, \nabla_x \vartheta) \cdot \nabla_x \vartheta}{\vartheta} \,\mathrm{d}x \,\mathrm{d}t \,\mathrm{d}s$$
$$- \int_{\tau-\delta}^{\tau+\delta} \int_0^s \int_{\mathbb{T}^d \setminus \Omega} \frac{\boldsymbol{q}(\vartheta_B, \nabla_x \vartheta_B) \cdot \nabla_x \vartheta_B}{\vartheta_B} \,\mathrm{d}x \,\mathrm{d}t \,\mathrm{d}s. \tag{4.15}$$

Our ultimate goal is to perform the limit in the last integral in (4.13), namely

$$\lim_{\varepsilon \to 0} \int_{\tau-\delta}^{\tau+\delta} \int_0^s \int_{\mathbb{T}^d} \frac{\boldsymbol{q}(\vartheta_\varepsilon, \nabla_x \vartheta_\varepsilon) \cdot \nabla_x \tilde{\vartheta}}{\vartheta_\varepsilon} \,\mathrm{d}x \,\mathrm{d}t \,\mathrm{d}s = \int_{\tau-\delta}^{\tau+\delta} \int_0^s \int_\Omega \frac{\boldsymbol{q}(\vartheta, \nabla_x \vartheta) \cdot \nabla_x \tilde{\vartheta}}{\vartheta} \,\mathrm{d}x \,\mathrm{d}t \,\mathrm{d}s$$
$$+ \int_{\tau-\delta}^{\tau+\delta} \int_0^s \int_{\mathbb{T}^d \setminus \Omega} \frac{\boldsymbol{q}(\vartheta_B, \nabla_x \vartheta_B) \cdot \nabla_x \vartheta_B}{\vartheta_B} \,\mathrm{d}x \,\mathrm{d}t \,\mathrm{d}s. \tag{4.16}$$

In view of the strong convergence of $(\vartheta_\varepsilon)_{\varepsilon > 0}$ and weak convergence of $(\nabla_x \vartheta_\varepsilon)_{\varepsilon > 0}$, it is enough to observe that the terms

$$\frac{\kappa(\vartheta_\varepsilon)}{\vartheta_\varepsilon} \nabla_x \vartheta_\varepsilon, \ \varepsilon > 0$$

are equi–integrable. Seeing that for small values of ϑ_ε we have $\frac{\kappa(\vartheta_\varepsilon)}{\vartheta_\varepsilon} \nabla_x \vartheta_\varepsilon \approx \nabla_x \log(\vartheta_\varepsilon)$ controlled by (3.13), we focus on

$$\vartheta_\varepsilon^{\beta-1} \nabla_x \vartheta_\varepsilon, \ \vartheta_\varepsilon \geq 1, \ \varepsilon > 0.$$

Writing

$$\vartheta_\varepsilon^{\beta-1} \nabla_x \vartheta_\varepsilon = \vartheta_\varepsilon^{\frac{\beta}{2}} \nabla_x \vartheta_\varepsilon^{\frac{\beta}{2}}$$

we observe, by virtue of the estimates (3.13), that it is enough to control the norm

$$\left\| \vartheta_\varepsilon^{\frac{\beta}{2}} \right\|_{L^q((0,T)\times\mathbb{T}^d)} \lesssim 1 \text{ for some } q > 2.$$

This is definitely possible on the set $(0,T)\times\left(\mathbb{T}^d \setminus \Omega\right)$ since $k+1 > \beta$. As for Ω, we have, by virtue of (3.13) and the standard Sobolev emebedding,

$$\left(\vartheta_\varepsilon^{\frac{\beta}{2}}\right)_{\varepsilon>0} \text{ bounded in } L^2\big(0,T;L^6(\Omega)\big),\ (\vartheta_\varepsilon)_{\varepsilon>0} \text{ bounded in } L^\infty(0,T;L^4(\Omega));$$

whence the desired conclusion follows by interpolation.

Plugging (4.14)–(4.16) in (4.13) we get

$$\begin{aligned}
&\int_{\tau-\delta}^{\tau+\delta}\int_\Omega \left(\frac{1}{2}\varrho|\boldsymbol{u}|^2 + \varrho e(\varrho,\vartheta) - \tilde\vartheta\varrho s(\varrho,\vartheta)\right)(s,\cdot)\,\mathrm{d}x\,\mathrm{d}s \\
&\quad + \int_{\tau-\delta}^{\tau+\delta}\int_0^s\int_\Omega \frac{\tilde\vartheta}{\vartheta}\left(\mathbb{S}(\vartheta,\mathbb{D}_x\boldsymbol{u}) : \mathbb{D}_x\boldsymbol{u} - \frac{\boldsymbol{q}(\vartheta,\nabla_x\vartheta)\cdot\nabla_x\vartheta_\varepsilon}{\vartheta}\right)\mathrm{d}x\,\mathrm{d}t\,\mathrm{d}s \\
&\quad \le 2\delta\int_\Omega\left(\frac{1}{2}\frac{|\boldsymbol{m}_0|^2}{\varrho_0} + \varrho_0 e(\varrho_0,S_0) - \tilde\vartheta(0,\cdot)S_0\right)\mathrm{d}x \\
&\qquad - \int_{\tau-\delta}^{\tau+\delta}\int_0^s\int_\Omega\left(\varrho s(\varrho,\vartheta)\Big(\partial_t\tilde\vartheta + \boldsymbol{u}\cdot\nabla_x\tilde\vartheta\Big) + \frac{\boldsymbol{q}(\vartheta,\nabla_x\vartheta)\cdot\nabla_x\tilde\vartheta}{\vartheta}\right)\mathrm{d}x\,\mathrm{d}t\,\mathrm{d}s
\end{aligned}$$

for any $\delta > 0$. Finally, we divide the above inequality by 2δ and let $\delta \to 0$ obtaining

$$\begin{aligned}
&\int_\Omega\left(\frac{1}{2}\varrho|\boldsymbol{u}|^2 + \varrho e(\varrho,\vartheta) - \tilde\vartheta\varrho s(\varrho,\vartheta)\right)(\tau,\cdot)\,\mathrm{d}x \\
&\quad + \int_0^\tau\int_\Omega \frac{\tilde\vartheta}{\vartheta}\left(\mathbb{S}(\vartheta,\mathbb{D}_x\boldsymbol{u}) : \mathbb{D}_x\boldsymbol{u} - \frac{\boldsymbol{q}(\vartheta,\nabla_x\vartheta)\cdot\nabla_x\vartheta_\varepsilon}{\vartheta}\right)\mathrm{d}x\,\mathrm{d}t \\
&\quad \le \int_\Omega\left(\frac{1}{2}\frac{|\boldsymbol{m}_0|^2}{\varrho_0} + \varrho_0 e(\varrho_0,S_0) - \tilde\vartheta(0,\cdot)S_0\right)\mathrm{d}x \\
&\qquad - \int_0^\tau\int_\Omega\left(\varrho s(\varrho,\vartheta)\Big(\partial_t\tilde\vartheta + \boldsymbol{u}\cdot\nabla_x\tilde\vartheta\Big) + \frac{\boldsymbol{q}(\vartheta,\nabla_x\vartheta)\cdot\nabla_x\tilde\vartheta}{\vartheta}\right)\mathrm{d}x\,\mathrm{d}t
\end{aligned}$$

for *a.a.* $\tau \in (0,T)$, which is nothing other than the ballistic energy inequality (2.22).

We have proved Theorem 2.3.

4.3. Time independent ϑ_B

Finally, we consider the time independent boundary temperature as specified in hypothesis (2.24). Under these circumstances, the main stumbling block is the fact that the strong convergence of the density outside Ω stated in (4.4) is no longer valid.

Fortunately, as ϑ_B is independent of time, the integrals over $\mathbb{T}^d\setminus\overline{\Omega}$ vanish in (4.11). Moreover, the convergence in (4.9) reads now

$$\begin{aligned}
\int_{\mathbb{T}^d}\left(\frac{1}{2}\frac{|\boldsymbol{m}_{0,\varepsilon}|^2}{\varrho_{0,\varepsilon}} + \varrho_{0,\varepsilon}e(\varrho_{0,\varepsilon},S_{0,\varepsilon}) - \tilde\vartheta(0,\cdot)S_{0,\varepsilon}\right)\mathrm{d}x \to \int_\Omega\left(\frac{1}{2}\frac{|\boldsymbol{m}_0|^2}{\varrho_0} + \varrho_0 e(\varrho_0,S_0) - \tilde\vartheta(0,\cdot)S_0\right)\mathrm{d}x \\
+ \int_{\mathbb{T}^d\setminus\Omega}(\varrho_0 e(\varrho_0,S_0) - \vartheta_B S_0)\,\mathrm{d}x. \qquad (4.17)
\end{aligned}$$

Next, in view of the strong convergence of the approximate solutions in Ω, we get

$$\begin{aligned}\liminf_{\varepsilon\to 0}\int_{\tau-\delta}^{\tau+\delta}\int_{\mathbb{T}^d}\left(\frac{1}{2}\varrho_\varepsilon|\boldsymbol{u}_\varepsilon|^2+\varrho_\varepsilon e(\varrho_\varepsilon,\vartheta_\varepsilon)-\tilde{\vartheta}\varrho_\varepsilon s(\varrho_\varepsilon,\vartheta_\varepsilon)\right)\mathrm{d}x\,\mathrm{d}t\\ \geq\int_{\tau-\delta}^{\tau+\delta}\int_{\Omega}\left(\frac{1}{2}\varrho|\boldsymbol{u}|^2+\varrho e(\varrho,\vartheta)-\tilde{\vartheta}\varrho s(\varrho,\vartheta)\right)\mathrm{d}x\,\mathrm{d}t\\ +\liminf_{\varepsilon\to 0}\int_{\tau-\delta}^{\tau+\delta}\int_{\mathbb{T}^d\setminus\Omega}\Big(\varrho_\varepsilon e(\varrho_\varepsilon,\vartheta_\varepsilon)-\vartheta_B\varrho_\varepsilon s(\varrho_\varepsilon,\vartheta_\varepsilon)\Big)\mathrm{d}x\,\mathrm{d}t.\end{aligned}\tag{4.18}$$

Finally, we first use Fatou's lemma to get

$$\liminf_{\varepsilon\to 0}\int_{\tau-\delta}^{\tau+\delta}\int_{\mathbb{T}^d\setminus\Omega}(\varrho_\varepsilon e(\varrho_\varepsilon,\vartheta_\varepsilon)-\vartheta_B\varrho_\varepsilon s(\varrho_\varepsilon,\vartheta_\varepsilon))\,\mathrm{d}x\geq\int_{\tau-\delta}^{\tau+\delta}\int_{\mathbb{T}^d\setminus\Omega}\left\langle\nu_{t,x};\tilde{\varrho}e\Big(\tilde{\varrho},\tilde{\vartheta}\Big)-\vartheta_B\tilde{\varrho}s\Big(\tilde{\varrho},\tilde{\vartheta}\Big)\right\rangle\mathrm{d}x\,\mathrm{d}t,$$

where $(\nu_{t,x})_{t\in(0,T),x\in\mathbb{T}^d\setminus\Omega}$ is a Young measure generated by the sequence $(\varrho_\varepsilon,\vartheta_\varepsilon)_{\varepsilon>0}$. In addition, as $\vartheta_\varepsilon\to\vartheta_B$ strongly, the Young measure can be written as

$$\nu_{t,x}=\delta_{\vartheta_B(x)}\otimes\omega_{t,x},$$

where $(\omega_{t,x})_{t\in(0,T),x\in\mathbb{T}^d\setminus\Omega}$ is the Young measure associated to $(\varrho_\varepsilon)_{\varepsilon>0}$. Accordingly,

$$\int_{\tau-\delta}^{\tau+\delta}\int_{\mathbb{T}^d\setminus\Omega}\left\langle\nu_{t,x};\tilde{\varrho}e\Big(\tilde{\varrho},\tilde{\vartheta}\Big)-\vartheta_B\tilde{\varrho}s\Big(\tilde{\varrho},\tilde{\vartheta}\Big)\right\rangle\mathrm{d}x\,\mathrm{d}t=\int_{\tau-\delta}^{\tau+\delta}\int_{\mathbb{T}^d\setminus\Omega}\langle\omega_{t,x};\tilde{\varrho}e(\tilde{\varrho},\vartheta_B)-\vartheta_B\tilde{\varrho}s(\tilde{\varrho},\vartheta_B)\rangle\,\mathrm{d}x\,\mathrm{d}t.$$

However, the function

$$\tilde{\varrho}\mapsto\tilde{\varrho}e(\tilde{\varrho},\vartheta_B)-\vartheta_B\tilde{\varrho}s(\tilde{\varrho},\vartheta_B)$$

is convex, see Chapter 2, Section 2.2.3 from [6]; whence, by Jensen's inequality,

$$\int_{\tau-\delta}^{\tau+\delta}\int_{\mathbb{T}^d\setminus\Omega}\langle\omega_{t,x};\tilde{\varrho}e(\tilde{\varrho},\vartheta_B)-\vartheta_B\tilde{\varrho}s(\tilde{\varrho},\vartheta_B)\rangle\,\mathrm{d}x\,\mathrm{d}t\geq 2\delta\int_{\mathbb{T}^d\setminus\Omega}(\varrho_0e(\varrho_0,\vartheta_B)-\vartheta_B\varrho_0s(\varrho_0,\vartheta_B))\,\mathrm{d}x.$$

Consequently, the last integrals in (4.17), (4.18) cancel out and the desired conclusion follows.

5. Finite volume simulations

The aim of this section is to illustrate convergence of the penalization method when simulating viscous compressible flows in complex geometries. To this end we apply the *finite volume method* (FV) that has been recently developed in [13] and analysed in [7]. In what follows we describe the FV method and present four numerical experiments for the Navier–Stokes–Fourier system. We will also study the experimental rate of convergence of the FV scheme with respect to both the discretization and the penalty parameters.

We consider for simplicity the perfect gas pressure law $p=\varrho\vartheta$, internal energy and entropy are given by $e=c_v\vartheta$, $s=\log\left(\frac{\vartheta^{c_v}}{\varrho}\right)=\frac{1}{\gamma-1}\log\left(\frac{p}{\varrho^\gamma}\right)$, respectively, where $c_v=\frac{1}{\gamma-1}$. In the numerical experiments presented below ϱ,ϑ are bounded from below and above. In this case theoretical results on the convergence of the penalization method can be obtained for the perfect gas pressure law as well.

5.1. Finite volume method

Our computational domain $\mathbb{T}^d \subset R^d$ is approximated by regular cuboids: finite volumes K of size h^d, where $h \in (0,1)$ is a mesh step. The piecewise constant numerical solutions $U_h^\varepsilon \equiv (\varrho_h^\varepsilon, \boldsymbol{u}_h^\varepsilon, \vartheta_h^\varepsilon)$ satisfy the following semi-discrete first order FV method

$$D_t \varrho_h^\varepsilon + \mathrm{div}_h^{\mathrm{up}} F(\varrho_h^\varepsilon, \boldsymbol{u}_h^\varepsilon) = 0, \tag{5.1a}$$

$$D_t \boldsymbol{m}_h^\varepsilon + \mathrm{div}_h^{\mathrm{up}} \boldsymbol{F}(\boldsymbol{m}_h^\varepsilon, \boldsymbol{u}_h^\varepsilon) + \nabla_h p_h^\varepsilon = 2\,\mathrm{div}_h(\mu_h^\varepsilon \mathbb{D}_h \boldsymbol{u}_h^\varepsilon) + \nabla_h(\lambda_h^\varepsilon\,\mathrm{div}_h\,\boldsymbol{u}_h^\varepsilon) + \varrho_h^\varepsilon \boldsymbol{g}_h^\varepsilon - \frac{1}{\varepsilon}\mathbb{1}_{\mathbb{T}^d\setminus\Omega}(K)\boldsymbol{u}_h^\varepsilon, \tag{5.1b}$$

$$D_t 0(\varrho_h^\varepsilon e_h^\varepsilon) + \mathrm{div}_h^{\mathrm{up}} F(\varrho_h^\varepsilon e_h^\varepsilon, \boldsymbol{u}_h^\varepsilon) + p_h^\varepsilon\,\mathrm{div}_h\,\boldsymbol{u}_h^\varepsilon = \mathrm{div}_h(\kappa_h^\varepsilon \nabla_h \vartheta_h^\varepsilon) + 2\mu_h^\varepsilon |\mathbb{D}_h \boldsymbol{u}_h^\varepsilon|^2 + \lambda_h^\varepsilon |\,\mathrm{div}_h\,\boldsymbol{u}_h^\varepsilon|^2 - \frac{1}{\varepsilon}\mathbb{1}_{\mathbb{T}^d\setminus\Omega}(K)|\vartheta_h^\varepsilon - \vartheta_B|^k(\vartheta_h^\varepsilon - \vartheta_B) \tag{5.1c}$$

with $\boldsymbol{m}_h^\varepsilon = \varrho_h^\varepsilon \boldsymbol{u}_h^\varepsilon$, $e_h^\varepsilon = c_v \vartheta_h^\varepsilon$, coefficients $\mu_h^\varepsilon = \mu(\vartheta_h^\varepsilon)$, $\lambda_h^\varepsilon = \lambda(\vartheta_h^\varepsilon)$, $\lambda(\vartheta) = \eta(\vartheta) - 2\mu(\vartheta)/d$, $\kappa_h^\varepsilon = \kappa(\vartheta_h^\varepsilon)$, and the characteristic function

$$\mathbb{1}_{\mathbb{T}^d\setminus\Omega}(K) = \begin{cases} 1, & \text{if } K_c \in \mathbb{T}^d \setminus \Omega, \\ 0, & \text{otherwise,} \end{cases}$$

where K_c is the gravity center of K. Function $\boldsymbol{g}_h^\varepsilon$ stands for a piecewise constant approximation of an external (gravitational) force.

Let us define the discrete operators and the numerical flux function used in the scheme (5.1). By $\overline{r_h}$ and $[\![r_h]\!]$ we denote the average and jump along a cell interface for any r_h piecewise constant function, respectively. The discrete differential operators div_h and ∇_h are adjoint operators defined on each finite volume K in the following way

$$(\mathrm{div}_h \boldsymbol{v}_h)_K = \sum_{\sigma\in\partial K} \frac{|\sigma|}{|K|}\overline{\boldsymbol{v}_h}\cdot\boldsymbol{n}, \qquad (\nabla_h r_h)_K = \sum_{\sigma\in\partial K} \frac{|\sigma|}{|K|}\overline{r_h}\boldsymbol{n}, \qquad \mathbb{D}_h r_h = \frac{1}{2}\big(\nabla_h r_h + (\nabla_h r_h)^t\big),$$

where $\boldsymbol{v}_h$ is a vector-valued piecewise constant function on $\mathbb{T}^d$, and $\boldsymbol{n}$ denotes an outer normal vector to ∂K. For flux approximation we apply the viscosity upwind numerical flux F_h defined by

$$F_h(r_h, \boldsymbol{v}_h) = Up[r_h, \boldsymbol{v}_h] - h^\alpha [\![r_h]\!], \quad 0 < \alpha < 1,$$
$$Up[r_h, \boldsymbol{v}_h] = \overline{r_h}\,\overline{\boldsymbol{v}_h}\cdot\mathbf{n} - \frac{1}{2}|\overline{\boldsymbol{v}_h}\cdot\mathbf{n}|[\![r_h]\!].$$

Moreover, we set

$$\big(\mathrm{div}_h^{\mathrm{up}} F(r_h, \boldsymbol{v}_h)\big)_K = \sum_{\sigma\in\partial K}\frac{|\sigma|}{|K|}F_h(r_h, \boldsymbol{v}_h).$$

For a vector-valued piecewise constant function $\boldsymbol{w}_h$ on $\mathbb{T}^d$ the discrete divergence $\mathrm{div}_h^{\mathrm{up}} \boldsymbol{F}(\boldsymbol{w}_h, \boldsymbol{v}_h)_K$ is defined componentwisely. See [13] for further details.

In our simulations we take the symbol D_t in (5.1) as the forward Euler discretization with the time step $\Delta t = 10^{-6}$. Initial data $(\varrho_{h,0}, \boldsymbol{u}_{h,0}, \vartheta_{h,0})$ are taken as piecewise constant projections of the exact initial data $(\varrho_0, \boldsymbol{u}_0, \vartheta_0)$ computed directly from $(\varrho_0, \boldsymbol{m}_0, S_0)$, *cf.* Theorem 2.3. Thus, $\boldsymbol{u}_0 = \frac{\boldsymbol{m}_0}{\varrho_0}$, $\varrho_0 > 0$ and $\vartheta_0 = \exp[(\gamma-1)(S_0/\varrho_0 + \log\varrho_0)]$. We set the transport coefficients and other parameters in (5.1),

$$\mu = \lambda = \kappa = 0.001,\ \gamma = 1.4,\ k = 6,\ \alpha = 0.6.$$

The computational domain $\mathbb{T}^2$ is taken as $[-1,1]^2$ applying the periodic boundary condition. Following the theoretical part, *cf.* Theorem 2.3 and Section 4.3, we will test two cases for the extension of the density outside the fluid domain Ω:

– constant density, *i.e.*

$$\mathbb{1}_{\mathbb{T}^d\setminus\Omega}\varrho_{h,0} = 1,$$

– "zero" density, *i.e.*

$$\mathbb{1}_{\mathbb{T}^d\setminus\Omega}\varrho_{h,0} = 0.01.$$

The latter is chosen as an approximation, since $\mathbb{1}_{\mathbb{T}^d\setminus\Omega}\varrho_{h,0} = 0$ is numerically unstable.

In the following, we present numerical solutions obtained by the FV method with the penalty parameter $\varepsilon = 10^{-m}, m = 1,\dots,4$ and mesh-size $h = 4/(10\times 2^n), n = 1,\dots,5$. Correspondingly, we compute three L^1-errors at the finial time T, *i.e.*

$$\begin{aligned}
E_1(U_h^\varepsilon) &= \left\|U_h^\varepsilon(T,\cdot) - U_{h_{\mathrm{ref}}}^\varepsilon(T,\cdot)\right\|_{L^1(\mathbb{T}^2)},\\
E_2(U_h^\varepsilon) &= \left\|U_h^\varepsilon(T,\cdot) - U_h^{\varepsilon_{\mathrm{ref}}}(T,\cdot)\right\|_{L^1(\mathbb{T}^2)},\\
E_3(U_h^\varepsilon) &= \left\|U_h^\varepsilon(T,\cdot) - U_{h_{\mathrm{ref}}}^{\varepsilon_{\mathrm{ref}}}(T,\cdot)\right\|_{L^1(\mathbb{T}^2)},
\end{aligned}$$

respectively, with $h_{\mathrm{ref}} = 4/(10\times 2^{-5})$, $\varepsilon_{\mathrm{ref}} = 10^{-4}$. We would like to point out that the error $E_1(U_h^\varepsilon)$ verifies the convergence rate of the FV method for a fixed penalization parameter ε while $E_2(U_h^\varepsilon)$ is used to study the convergence rate of the penalization technique for a fixed h. Further, we calculate $E_3(U_h^\varepsilon)$ with the parameter pair $(h,\varepsilon(h)) = (4/(10\times 2^m), 10^{-m}), m = 1,\dots,4$ to investigate the convergence showed in Theorem 2.3.

5.2. Experiment 1: Ring domain – constant density outside Ω

In this experiment we consider the physical fluid domain to be a ring, *i.e.* $\Omega \equiv B_{0.7}\setminus B_{0.2}$, where $B_r = \{x\in R^2 \mid |x|\le r\}$. The initial data are given by

$$(\varrho,\boldsymbol{u},\vartheta)(0,x) = \begin{cases} (1,0,0,1), & x\in B_{0.2},\\ \left(1, \frac{\sin(4\pi(|x|-0.2))x_2}{|x|}, -\frac{\sin(4\pi(|x|-0.2))x_1}{|x|}, 0.2+4|x|\right), & x\in\Omega\equiv B_{0.7}\setminus B_{0.2},\\ (1,0,0,3), & x\in\mathbb{T}^2\setminus B_{0.7}. \end{cases}$$

The final time is taken as $T = 0.1$. Figure 1 shows all three types of errors, *i.e.* with respect to the mesh-size h, $E_1(U_h^\varepsilon)$, with respect to the penalization parameter ε, $E_2(U_h^\varepsilon)$, as well as with respect to $(h,\varepsilon(h)) = (4/(10\times 2^m), 10^{-m})$, $E_3(U_h^\varepsilon)$. Experimental convergence study indicates that the convergence rate in all cases is 1. Effects of different penalization parameters $\varepsilon = 10^{-1},\dots,10^{-4}$ are illustrated in Figure 2, which depicts the numerical solutions on the mesh with 80^2 cells.

5.3. Experiment 2: Ring domain – zero density outside Ω

In this experiment we use a small initial density outside the fluid domain which approximates the case of zero density outside Ω studied in the theoretical part. The rest of the set up is the same as in Experiment 1, the initial data read

$$(\varrho,\boldsymbol{u},\vartheta)(0,x) = \begin{cases} \left(10^{-2},0,0,1\right), & x\in B_{0.2},\\ \left(1, \frac{\sin(4\pi(|x|-0.2))x_2}{|x|}, -\frac{\sin(4\pi(|x|-0.2))x_1}{|x|}, 0.2+4|x|\right), & x\in\Omega\equiv B_{0.7}\setminus B_{0.2},\\ \left(10^{-2},0,0,3\right), & x\in\mathbb{T}^2\setminus B_{0.7}. \end{cases}$$

Analogously as above, Figure 3 presents the errors $E_i(U_h^\varepsilon), i = 1,2,3$. The convergence rate 1 with respect to h, ε and $(h,\varepsilon(h)) = (4/(10\times 2^m), 10^{-m})$ is numerically confirmed. Figure 4 demonstrates the influence of the penalization parameter $\varepsilon = 10^{-1},\dots,10^{-4}$ in the numerical solution computed on the mesh with 80^2 cells. Due to small value of the outside density, the fluid tends to flow out of the fluid region Ω which acts against the penalization and consequently leads to small oscillation near the boundary.

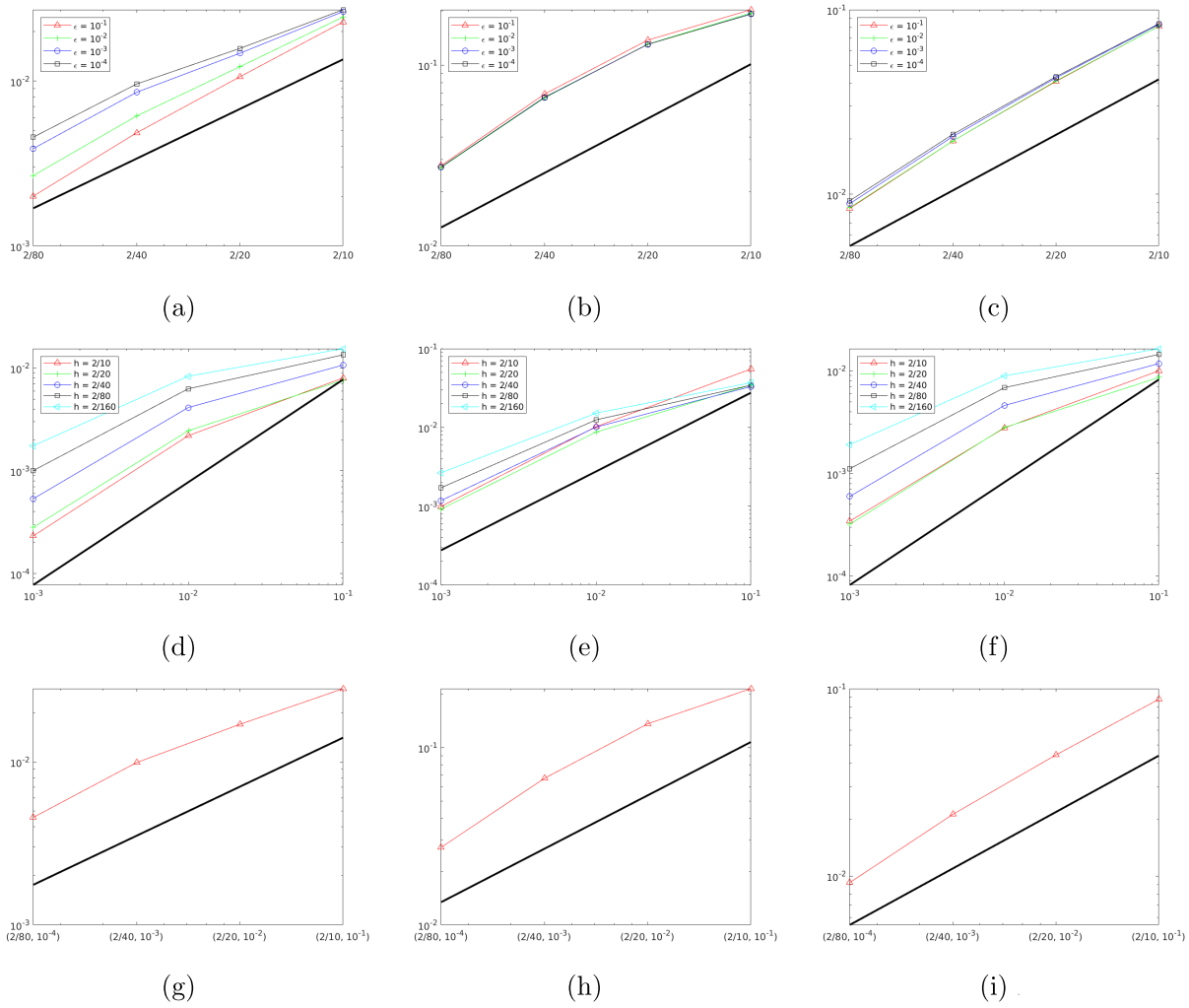

FIGURE 1. Experiment 1: Errors $E_i(U_h^\varepsilon), i = 1, 2, 3$. The solid line without any marker in the figures denote the reference slope of h (*top*), ε (*middle*) and h (*bottom*). (a) $E_1(U_h^\varepsilon) - \varrho$. (b) $E_1(U_h^\varepsilon) - \boldsymbol{u}$. (c) $E_1(U_h^\varepsilon) - \vartheta$. (d) $E_2(U_h^\varepsilon) - \varrho$. (e) $E_2(U_h^\varepsilon) - \boldsymbol{u}$. (f) $E_2(U_h^\varepsilon) - \vartheta$. (g) $E_3(U_h^\varepsilon) - \varrho$. (h) $E_3(U_h^\varepsilon) - \boldsymbol{u}$. (i) $E_3(U_h^\varepsilon) - \vartheta$.

5.4. Experiment 3: Complex domain – zero density outside Ω

We consider the same initial data as in the previous experiment but choose a more complicated geometry of the fluid domain $\Omega \equiv \hat{B}_{0.7} \setminus S_{0.2}$, where

$$\hat{B}_{0.7} := \left\{ x \in R^2 \;\middle|\; |x| \leq (0.7 + \delta) + \delta \cos(8\phi),\ \tan(\phi) = \frac{x}{y} \right\}, \quad S_{0.2} = \left\{ x \in R^2 \;\middle|\; |x_1| + |x_2| \leq 0.2 \right\}.$$

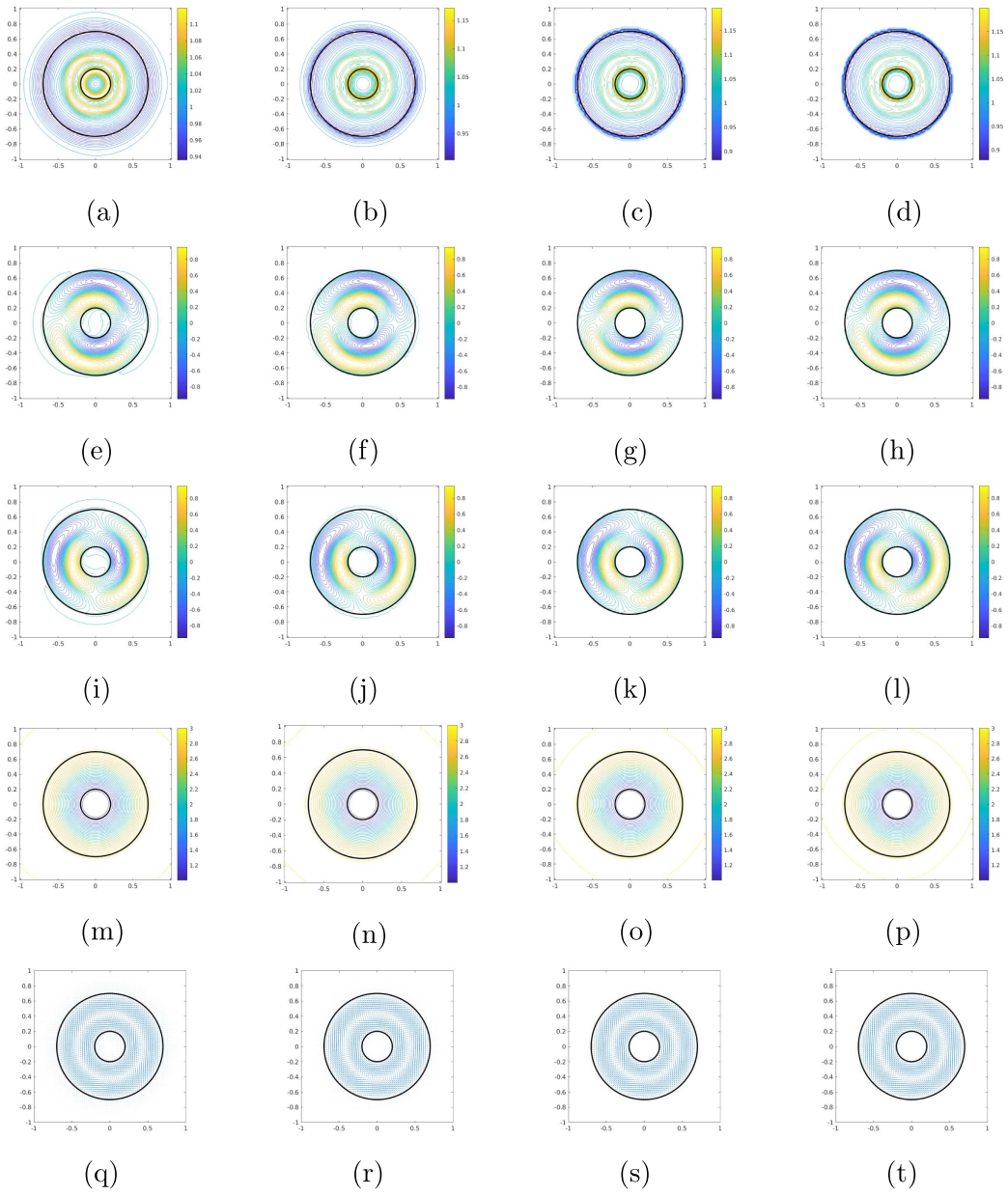

FIGURE 2. Experiment 1: Numerical solutions U_h^ε obtained with $h = 2/80$ and $\varepsilon = 10^{-1}, \ldots, 10^{-4}$. (a) $\varrho, \varepsilon = 10^{-1}$. (b) $\varrho, \varepsilon = 10^{-2}$. (c) $\varrho, \varepsilon = 10^{-3}$. (d) $\varrho, \varepsilon = 10^{-4}$. (e) $u_1, \varepsilon = 10^{-1}$. (f) $u_1, \varepsilon = 10^{-2}$. (g) $u_1, \varepsilon = 10^{-3}$. (h) $u_1, \varepsilon = 10^{-4}$. (i) $u_2, \varepsilon = 10^{-1}$. (j) $u_2, \varepsilon = 10^{-2}$. (k) $u_2, \varepsilon = 10^{-3}$. (l) $u_2, \varepsilon = 10^{-4}$. (m) $\vartheta, \varepsilon = 10^{-1}$. (n) $\vartheta, \varepsilon = 10^{-2}$. (o) $\vartheta, \varepsilon = 10^{-3}$. (p) $\vartheta, \varepsilon = 10^{-4}$. (q) $\boldsymbol{u}, \varepsilon = 10^{-1}$. (r) $\boldsymbol{u}, \varepsilon = 10^{-2}$. (s) $\boldsymbol{u}, \varepsilon = 10^{-3}$. (t) $\boldsymbol{u}, \varepsilon = 10^{-4}$.

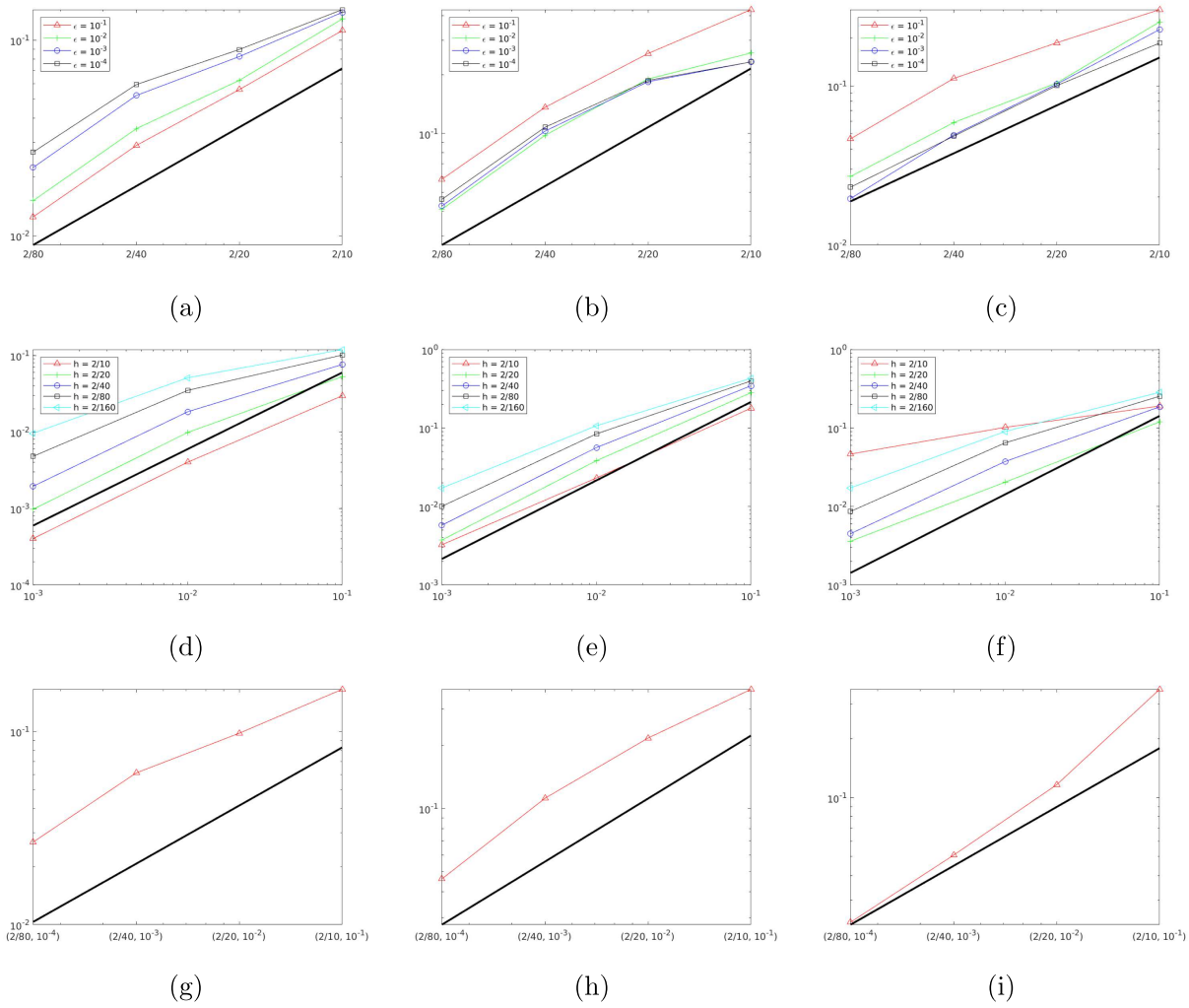

FIGURE 3. Experiment 2: Errors $E_i(U_h^\varepsilon), i = 1, 2, 3$. The solid line without any marker in the figures denote the reference slope of h (*top*), ε (*middle*) and h (*bottom*). (a) $E_1(U_h^\varepsilon) - \varrho$. (b) $E_1(U_h^\varepsilon) - \boldsymbol{u}$. (c) $E_1(U_h^\varepsilon) - \vartheta$. (d) $E_2(U_h^\varepsilon) - \varrho$. (e) $E_2(U_h^\varepsilon) - \boldsymbol{u}$. (f) $E_2(U_h^\varepsilon) - \vartheta$. (g) $E_3(U_h^\varepsilon) - \varrho$. (h) $E_3(U_h^\varepsilon) - \boldsymbol{u}$. (i) $E_3(U_h^\varepsilon) - \vartheta$.

Note that Ω has only Lipschitz-continuous boundary $\partial\Omega$. The initial data are given by

$$(\varrho, \boldsymbol{u}, \vartheta)(0, x) = \begin{cases} \big(10^{-2}, 0, 0, 1\big), & x \in S_{0.2}, \\ (1, 0, 0, 1), & x \in B_{0.2} \setminus S_{0.2}, \\ \Big(1, \frac{\sin(4\pi(|x|-0.2))x_2}{|x|}, -\frac{\sin(4\pi(|x|-0.2))x_1}{|x|}, 0.2 + 4|x|\Big), & x \in \Omega \equiv B_{0.7} \setminus B_{0.2}, \\ (1, 0, 0, 3), & x \in \hat{B}_{0.7} \setminus B_{0.7}, \\ \big(10^{-2}, 0, 0, 3\big), & x \in \mathbb{T}^2 \setminus \hat{B}_{0.7}. \end{cases}$$

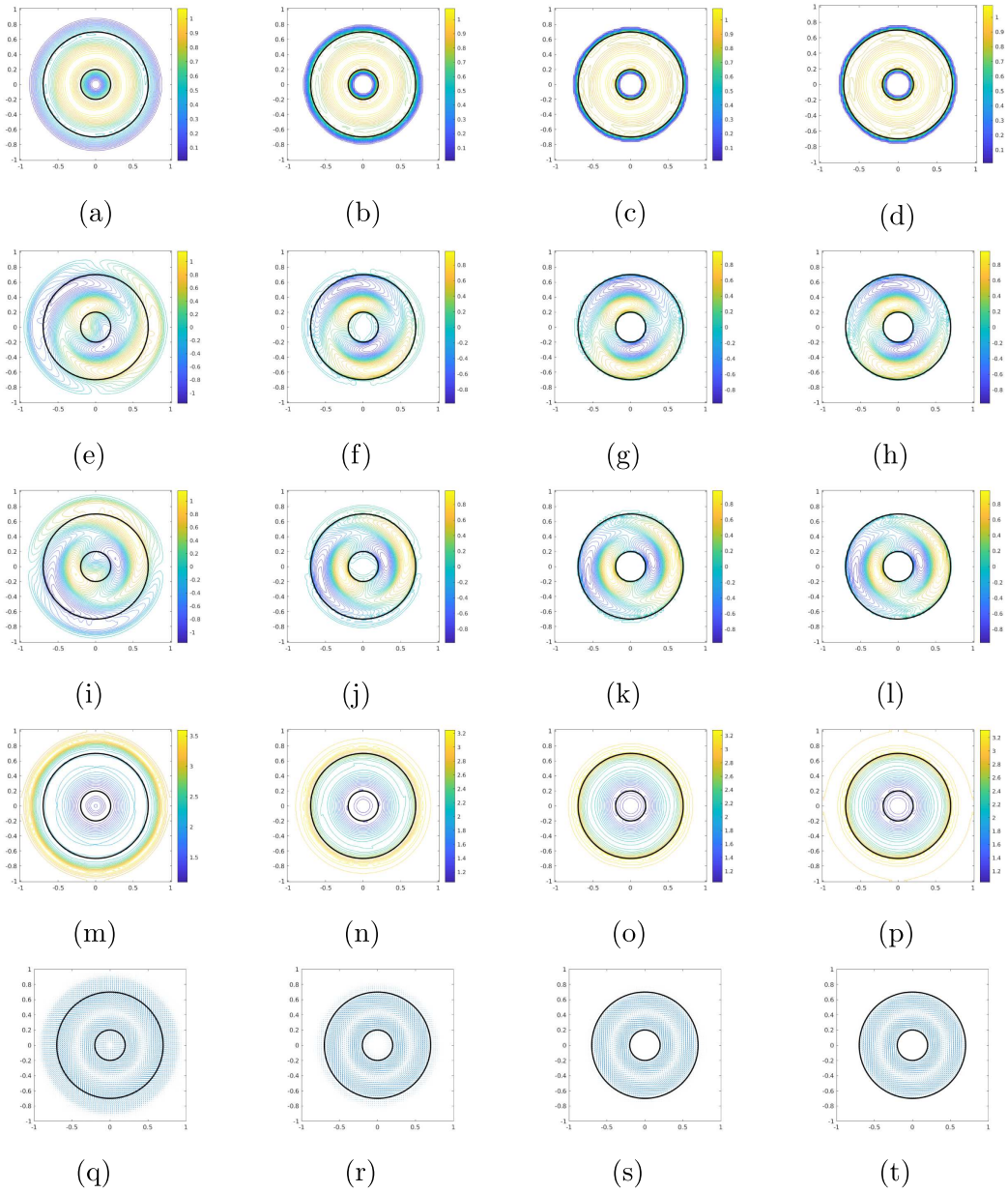

FIGURE 4. Experiment 2: Numerical solutions U_h^ε obtained with $h = 2/80$ and $\varepsilon = 10^{-1}, \ldots, 10^{-4}$. (a) $\varrho, \varepsilon = 10^{-1}$. (b) $\varrho, \varepsilon = 10^{-2}$. (c) $\varrho, \varepsilon = 10^{-3}$. (d) $\varrho, \varepsilon = 10^{-4}$. (e) $u_1, \varepsilon = 10^{-1}$. (f) $u_1, \varepsilon = 10^{-2}$. (g) $u_1, \varepsilon = 10^{-3}$. (h) $u_1, \varepsilon = 10^{-4}$. (i) $u_2, \varepsilon = 10^{-1}$. (j) $u_2, \varepsilon = 10^{-2}$. (k) $u_2, \varepsilon = 10^{-3}$. (l) $u_2, \varepsilon = 10^{-4}$. (m) $\vartheta, \varepsilon = 10^{-1}$. (n) $\vartheta, \varepsilon = 10^{-2}$. (o) $\vartheta, \varepsilon = 10^{-3}$. (p) $\vartheta, \varepsilon = 10^{-4}$. (q) $\boldsymbol{u}, \varepsilon = 10^{-1}$. (r) $\boldsymbol{u}, \varepsilon = 10^{-2}$. (s) $\boldsymbol{u}, \varepsilon = 10^{-3}$. (t) $\boldsymbol{u}, \varepsilon = 10^{-4}$.

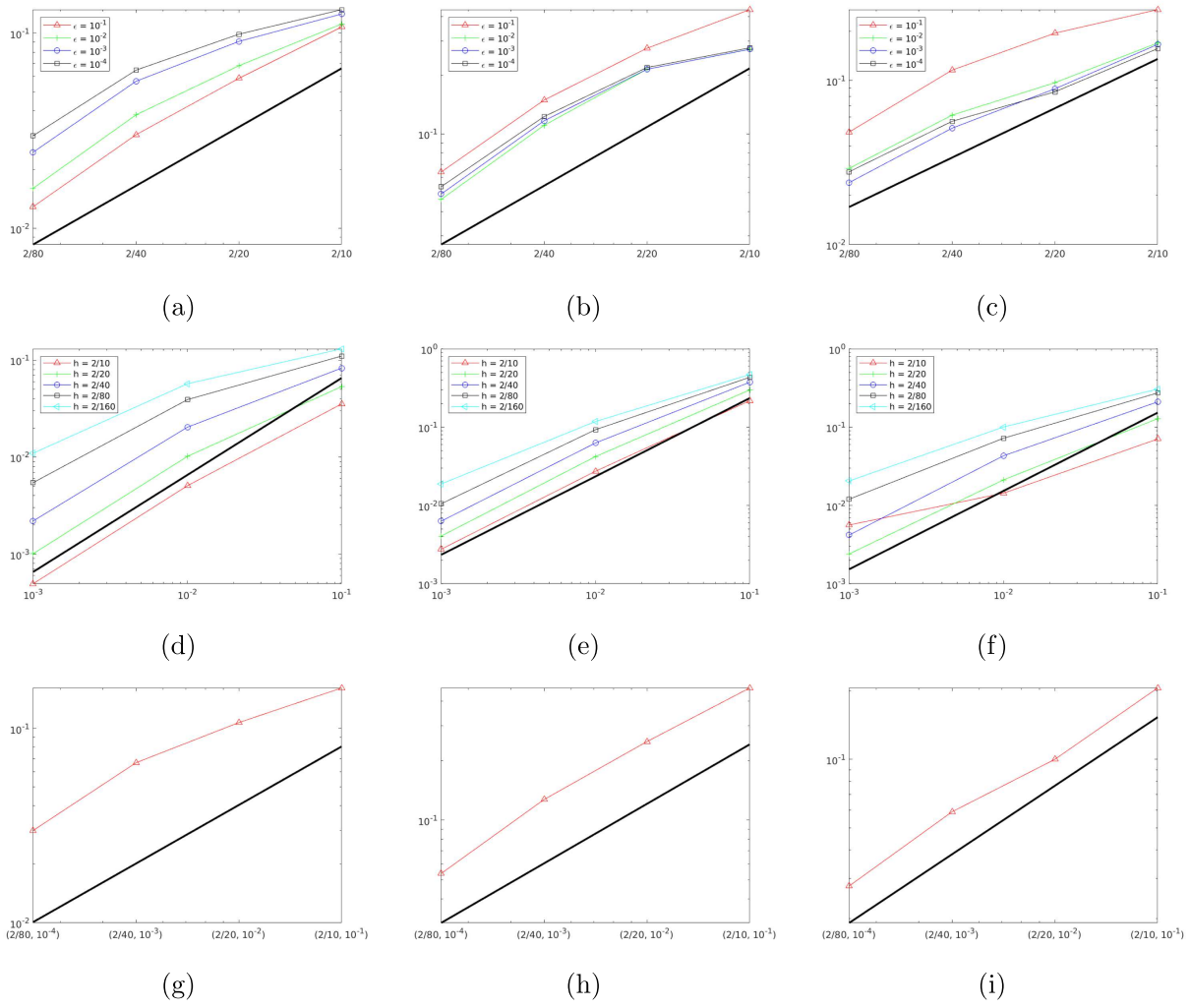

FIGURE 5. Experiment 3: Errors $E_i(U_h^\varepsilon), i = 1, 2, 3$. The solid line without any marker in the figures denote the reference slope of h (*top*), ε (*middle*) and h (*bottom*). (a) $E_1(U_h^\varepsilon) - \varrho$. (b) $E_1(U_h^\varepsilon) - \boldsymbol{u}$. (c) $E_1(U_h^\varepsilon) - \vartheta$. (d) $E_2(U_h^\varepsilon) - \varrho$. (e) $E_2(U_h^\varepsilon) - \boldsymbol{u}$. (f) $E_2(U_h^\varepsilon) - \vartheta$. (g) $E_3(U_h^\varepsilon) - \varrho$. (h) $E_3(U_h^\varepsilon) - \boldsymbol{u}$. (i) $E_3(U_h^\varepsilon) - \vartheta$.

In the simulations we set $\delta = 0.05$ and $T = 0.1$. Figure 5 demonstrates that the experimental convergence rates with respect to mesh size h, penalization parameter ε and pair $(h, \varepsilon(h)) = (4/(10 \times 2^m), 10^{-m})$ are of the first order. Figure 6 illustrates the effects of different penalization parameters $\varepsilon = 10^{-1}, \ldots, 10^{-4}$ on the numerical solutions computed on the mesh with 80^2 cells.

We can observe some oscillations near the inner and outer boundaries, whereas the oscillations at the outer boundary are larger than in Experiment 2. Due to small outside density the fluid flows outside, meanwhile the temperature pushes the fluid to flow to the center. Consequently, due to the complex geometry of the fluid domain, the oscillations become more visible and vortex structure arises. Interestingly, even that the oscillations are present, the penalization method still converges with rate 1, which is consistent with our theoretical analysis.

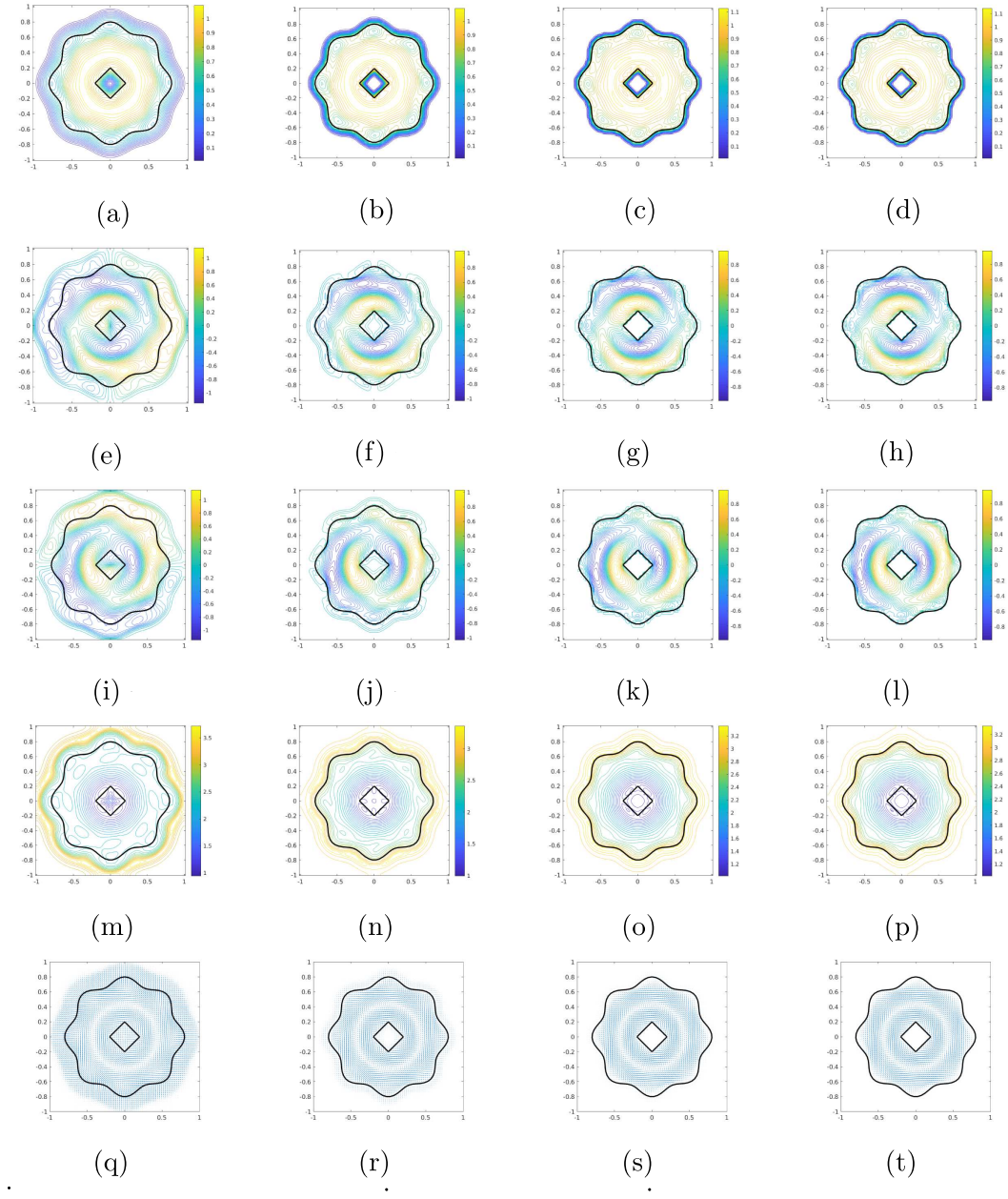

FIGURE 6. Experiment 3: Numerical solutions U_h^ε obtained with $h = 2/80$ and $\varepsilon = 10^{-1}, \ldots, 10^{-4}$. (a) $\varrho, \varepsilon = 10^{-1}$. (b) $\varrho, \varepsilon = 10^{-2}$. (c) $\varrho, \varepsilon = 10^{-3}$. (d) $\varrho, \varepsilon = 10^{-4}$. (e) $u_1, \varepsilon = 10^{-1}$. (f) $u_1, \varepsilon = 10^{-2}$. (g) $u_1, \varepsilon = 10^{-3}$. (h) $u_1, \varepsilon = 10^{-4}$. (i) $u_2, \varepsilon = 10^{-1}$. (j) $u_2, \varepsilon = 10^{-2}$. (k) $u_2, \varepsilon = 10^{-3}$. (l) $u_2, \varepsilon = 10^{-4}$. (m) $\vartheta, \varepsilon = 10^{-1}$. (n) $\vartheta, \varepsilon = 10^{-2}$. (o) $\vartheta, \varepsilon = 10^{-3}$. (p) $\vartheta, \varepsilon = 10^{-4}$. (q) $\boldsymbol{u}, \varepsilon = 10^{-1}$. (r) $\boldsymbol{u}, \varepsilon = 10^{-2}$. (s) $\boldsymbol{u}, \varepsilon = 10^{-3}$. (t) $\boldsymbol{u}, \varepsilon = 10^{-4}$.

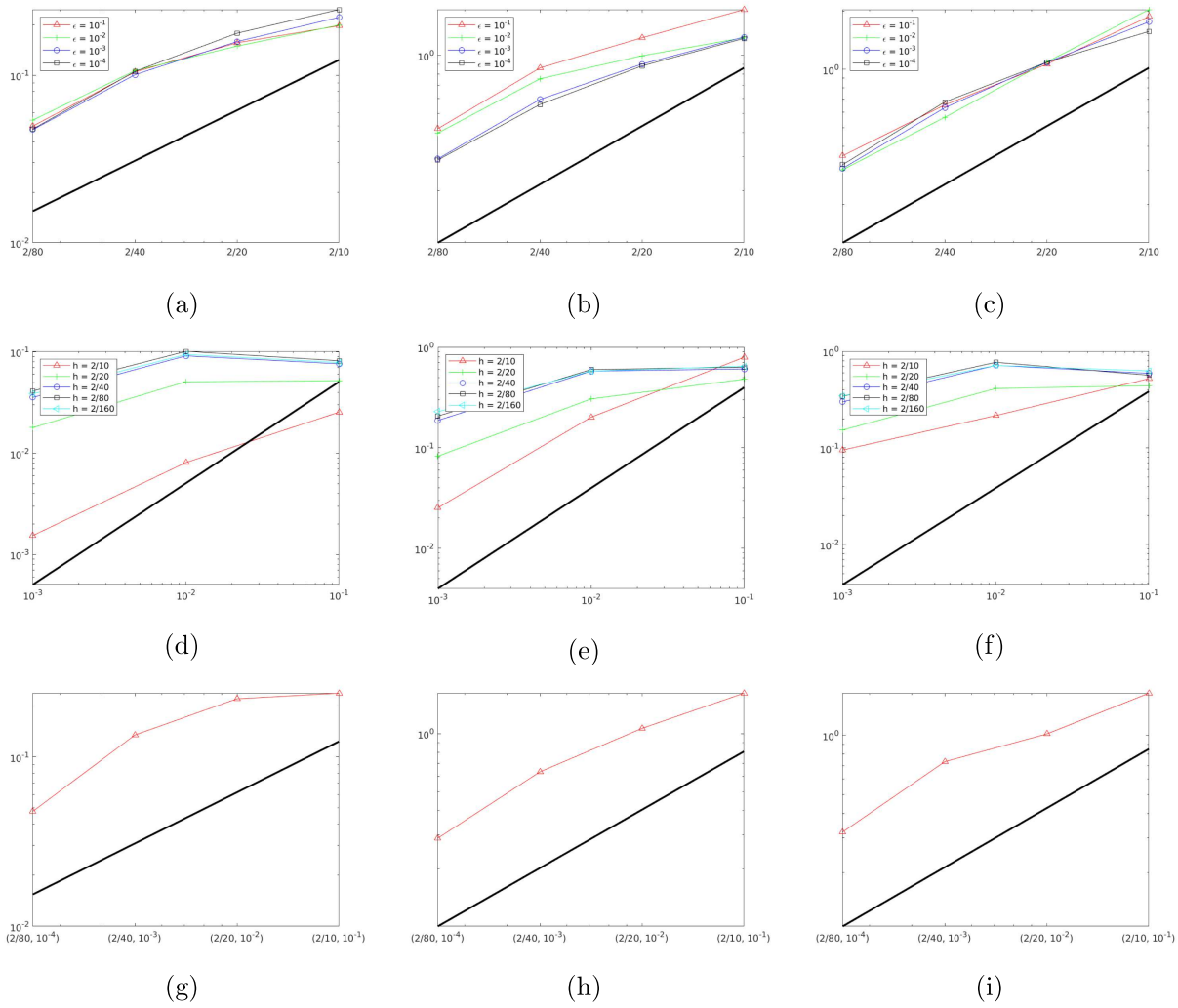

FIGURE 7. Experiment 4: Errors $E_i(U_h^\varepsilon), i = 1, 2, 3$. The solid line without any marker in the figures denote the reference slope of h (*top*), ε (*middle*) and h (*bottom*). (a) $E_1(U_h^\varepsilon) - \varrho$. (b) $E_1(U_h^\varepsilon) - \boldsymbol{u}$. (c) $E_1(U_h^\varepsilon) - \vartheta$. (d) $E_2(U_h^\varepsilon) - \varrho$. (e) $E_2(U_h^\varepsilon) - \boldsymbol{u}$. (f) $E_2(U_h^\varepsilon) - \vartheta$. (g) $E_3(U_h^\varepsilon) - \varrho$. (h) $E_3(U_h^\varepsilon) - \boldsymbol{u}$. (i) $E_3(U_h^\varepsilon) - \vartheta$.

5.5. Experiment 4: Ring domain – zero density outside Ω, non-zero gravity force

In the last experiment we extend the setting of Experiment 2 by adding an external force pointing to the center (0,0) defined by

$$\mathbf{g} = \left(-100\frac{x_1}{|x|}, -100\frac{x_2}{|x|}\right).$$

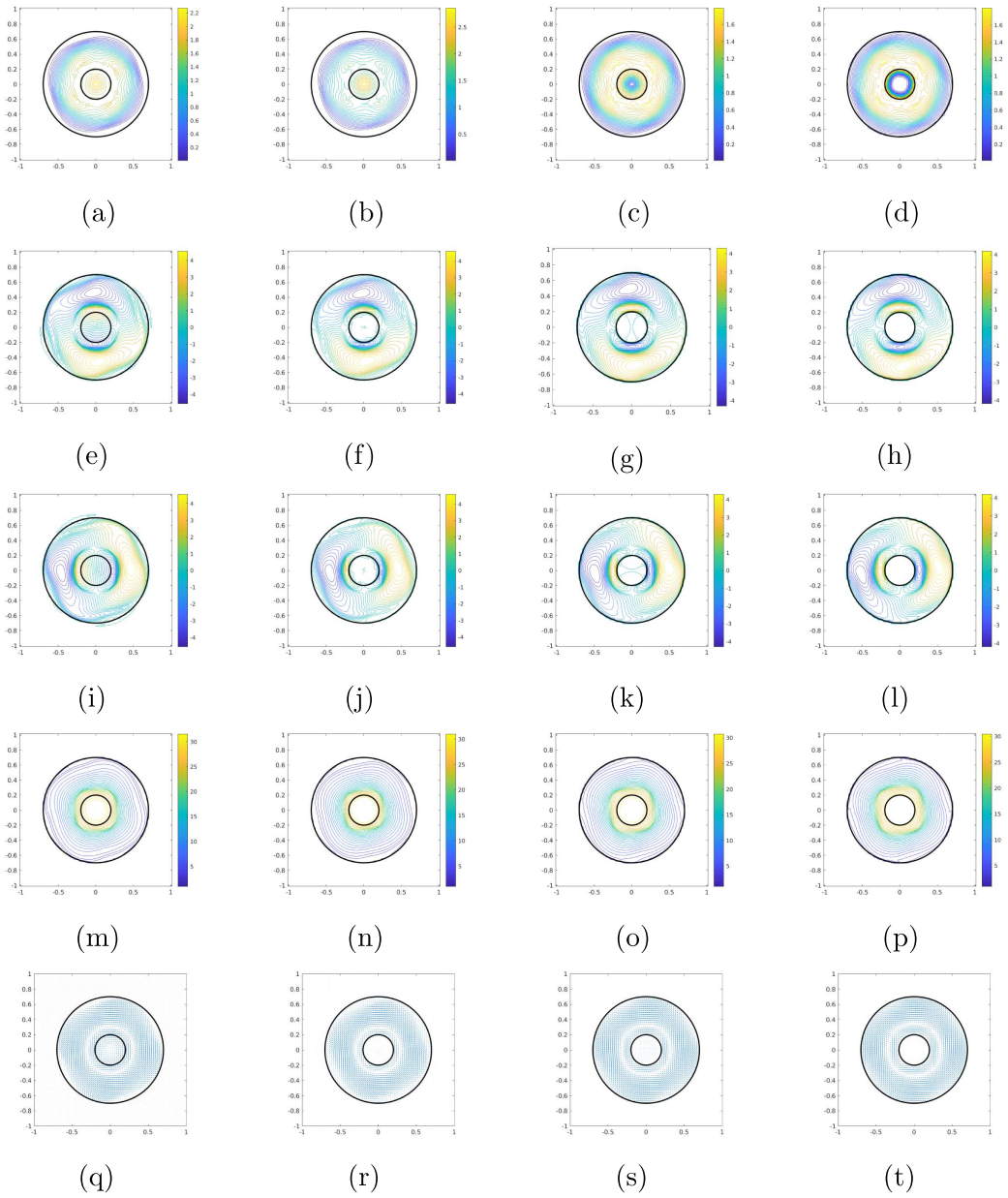

FIGURE 8. Experiment 4: Numerical solutions U_h^ε obtained with $h = 2/80$ and $\varepsilon = 10^{-1}, \ldots, 10^{-4}$. (a) $\varrho, \varepsilon = 10^{-1}$. (b) $\varrho, \varepsilon = 10^{-2}$. (c) $\varrho, \varepsilon = 10^{-3}$. (d) $\varrho, \varepsilon = 10^{-4}$. (e) $u_1, \varepsilon = 10^{-1}$. (f) $u_1, \varepsilon = 10^{-2}$. (g) $u_1, \varepsilon = 10^{-3}$. (h) $u_1, \varepsilon = 10^{-4}$. (i) $u_2, \varepsilon = 10^{-1}$. (j) $u_2, \varepsilon = 10^{-2}$. (k) $u_2, \varepsilon = 10^{-3}$. (l) $u_2, \varepsilon = 10^{-4}$. (m) $\vartheta, \varepsilon = 10^{-1}$. (n) $\vartheta, \varepsilon = 10^{-2}$. (o) $\vartheta, \varepsilon = 10^{-3}$. (p) $\vartheta, \varepsilon = 10^{-4}$. (q) $\boldsymbol{u}, \varepsilon = 10^{-1}$. (r) $\boldsymbol{u}, \varepsilon = 10^{-2}$. (s) $\boldsymbol{u}, \varepsilon = 10^{-3}$. (t) $\boldsymbol{u}, \varepsilon = 10^{-4}$.

In order to observe interesting phenomena the initial data are taken as

$$(\varrho,\boldsymbol{u},\vartheta)(0,x) = \begin{cases} (10^{-2},0,0,30), & x\in B_{0.2},\\ \Big(1,\frac{5\sin(4\pi(|x|-0.2))x_2}{|x|},-\frac{5\sin(4\pi(|x|-0.2))x_1}{|x|},41.6-58|x|\Big), & x\in\Omega\equiv B_{0.7}\setminus B_{0.2},\\ (10^{-2},0,0,1), & x\in\mathbb{T}^2\setminus B_{0.7}. \end{cases}$$

The final time is set to $T=0.2$.

The errors $E_i(U_h^\varepsilon), i=1,2,3$ are plotted in Figure 7. The results indicate that the numerical solutions converge with respect to h, ε and pair $(h,\varepsilon(h))=(4/(10\times 2^m),10^{-m})$ with rate nearly 1, 1/2, and 1, respectively. The numerical solutions for different penalization parameters $\varepsilon=10^{-1},\dots,10^{-4}$ on the mesh of 80^2 cells are shown in Figure 8.

Comparing these results with those of previous Experiments we can see oscillatory fluid behaviour which is due to the development of the so-called Rayleigh-Bénard convection rolls. These are visible in the density plots in Figure 8 and arise due to the temperate gradient acting against the outer force, see [14] for more details.

In summary, we have demonstrated experimentally that the penalization method (1.5)–(1.7) is robust and efficient. Penalized numerical solutions $(\rho_h^\varepsilon,\boldsymbol{u}_h^\varepsilon,\vartheta_h^\varepsilon)_{h\searrow 0,\varepsilon\searrow 0}$ converge to an exact solution $(\varrho,\boldsymbol{u},\vartheta)$ of the Dirichlet boundary problem. We have tested experimentally the strong convergence with respect to $L^1(\mathbb{T}^2)$-norm. In future our goal will be to extend theoretical analysis presented in this paper to the FV method (5.1) and prove rigorously its convergence with respect to both parameters, the discretization parameter h as well as the penalization parameter ε.

6. Conclusion

In the present paper we have studied convergence of a penalization method for the Navier–Stokes–Fourier system with the Dirichlet boundary conditions. The physical fluid domain is embedded into a large cube on which the periodic boundary conditions are imposed. The penalty terms act as the friction term in the momentum and the sink/source term in the internal energy balance, respectively. We have discussed two cases with zero and non-zero density outside of the physical fluid domain. In Theorem 2.3 we have shown that the penalized solutions converge to a weak solution of the Dirichlet problem. For domains with rough (Lipschitz) boundaries the existence of a global weak solution was an open problem. The key ingredient of the convergence analysis is the use of the ballistic energy inequality (3.3) as a source of uniform bounds, and the limiting process discussed in Section 4.2.

The penalization approach is also very suitable when fluid flow has to be simulated in complicated geometries. Clearly, to generate a good and fitted mesh for complex domains is time-consuming. Our penalization approach does not require any complicated meshes and it is enough to work with regular rectangular grids. Numerical experiments presented in Section 5 illustrate the main ideas of theoretical analysis and demonstrate the efficiency of our penalization technique in complex geometries.

Acknowledgements. We would like to thank Dr. Bangwei She (Prague/Beijing) for fruitful discussions on the numerical method and numerical results. The work of D.B., E.F. and H.M. was partially supported by the Czech Sciences Foundation (GAČR), Grant Agreement 21-02411S. The Institute of Mathematics of the Academy of Sciences of the Czech Republic is supported by RVO:67985840. M.L. has been funded by the Deutsche Forschungsgemeinschaft (DFG, German Research Foundation) – Project number 233630050 – TRR 146 as well as by TRR 165 Waves to Weather. She is grateful to the Gutenberg Research College and Mainz Institute of Multiscale Modelling for supporting her research. The research of Y.Y. was funded by Sino-German (CSC-DAAD) Postdoc Scholarship Program in 2020 – Project number 57531629.

References

[1] R. Beyer and R.J. LeVeque, Analysis of a one-dimensional model for the immersed boundary method. *SIAM J. Numer. Anal.* **29** (1992) 332–364.

[2] V. Bruneau, A. Doradoux and P. Fabrie, Convergence of a vector penalty projection scheme for the Navier Stokes equations with moving body. *ESAIM: Math. Model. Numer. Anal.* **52** (2018) 1417–1436.
[3] N. Chaudhuri and E. Feireisl, Navier–Stokes–Fourier system with Dirichlet boundary conditions. (2021). DOI: 10.1080/00036811.2021.1992396.
[4] P.A. Davidson, Turbulence: An Introduction for Scientists and Engineers. Oxford University Press, Oxford (2004).
[5] E. Feireisl and A. Novotný, Weak–strong uniqueness property for the full Navier–Stokes-Fourier system. *Arch. Ration. Mech. Anal.* **204** (2012) 683–706.
[6] E. Feireisl and A. Novotný, Singular Limits in Thermodynamics of Viscous Fluids, 2nd edition. *Advances in Mathematical Fluid Mechanics*. Birkhäuser (2017).
[7] E. Feireisl, M. Lukáčová-Medviďová, H. Mizerová and B. She, On the convergence of a finite volume method for the Navier–Stokes–Fourier system. *IMA J. Numer. Anal.* **41** (2021) 2388–2422.
[8] R. Glowinski, T.-W. Pan and J. Périaux, A fictitious domain method for Dirichlet problem and applications. *Comput. Methods Appl. Mech. Eng.* **111** (1994) 283–303.
[9] R. Glowinski, T.-W. Pan and J. Périaux, A fictitious domain method for external incompressible viscous flow modeled by Navier–Stokes equations. *Comput. Methods Appl. Mech. Eng.* **112** (1994) 133–148.
[10] J.S. Hesthaven, A stable penalty method for the compressible Navier–Stokes equations. II. One-dimensional domain decomposition schemes. *SIAM J. Sci. Comput.* **18** (1997) 658–685.
[11] J.S. Hesthaven, A stable penalty method for the compressible Navier–Stokes equations. III. Multidimensional domain decomposition schemes. *SIAM J. Sci. Comput.* **20** (1998) 62–93.
[12] M.A. Hyman, Non-iterative numerical solution of boundary-value problems. *Appl. Sci. Res. Sec. B* **2** (1952) 325–351.
[13] M. Lukáčová-Medviďová, H. Mizerová and B. She, New invariant domain preserving finite volume schemes for compressible flows. In: Recent Advances in Numerical Methods for Hyperbolic PDE Systems. Springer (2021) 131–153.
[14] P. Manneville, Rayleigh-Bénard convection: thirty years of experimental, theoretical, and modeling work. In: Dynamics of Spatio-temporal Cellular Structures, edited by I. Mutabazi, J. E. Wesfreid and E. Guyon. Springer (2006) 41–64.
[15] B. Maury, Numerical analysis of a finite element/volume penalty method. *SIAM J. Numer. Anal.* **47** (2009) 1126–1148.
[16] D. Medková, Boundary Value Problems on Bounded and Unbounded Lipschitz Domains. Springer-Verlag, Cham (2018).
[17] C.S. Peskin, Flow patterns around heart valves: a numerical method. *J. Comput. Phys.* **10** (1972) 252–271.
[18] C.S. Peskin, The immersed boundary method. *Acta Numer.* **11** (2002) 479–517.
[19] N. Saito and G. Zhou, Analysis of the fictitious domain method with an L^2-penalty for elliptic problems. *Numer. Funct. Anal. Optim.* **36** (2015) 501–527.
[20] S. Zhang, A domain embedding method for mixed boundary value problems. *C. R. Math. Acad. Sci. Paris* **343** (2006) 287–290.
[21] G. Zhou and N. Saito, Analysis of the fictitious domain method with penalty for elliptic problems. *Jpn. J. Ind. Appl. Math.* **31** (2014) 57–85.